

Berry opto-electronics: new tools for engineering light-matter interaction

Justin Song

Graphene 2017, Barcelona

*Institute of High Performance Computing, A*STAR &
Division of Physics and Applied Physics, Nanyang Technological University (Singapore)*

Funding:

**NATIONAL
RESEARCH
FOUNDATION**

Plan

Part I.

Giant Hall photoconductivity

gapped Dirac materials with a narrow gap yield Hall photoconductivity order $\sim e^2/h$; access to new “Berry” transport regime

JS, Kats, Nano Letters (2016)

if we have time:

Part II.

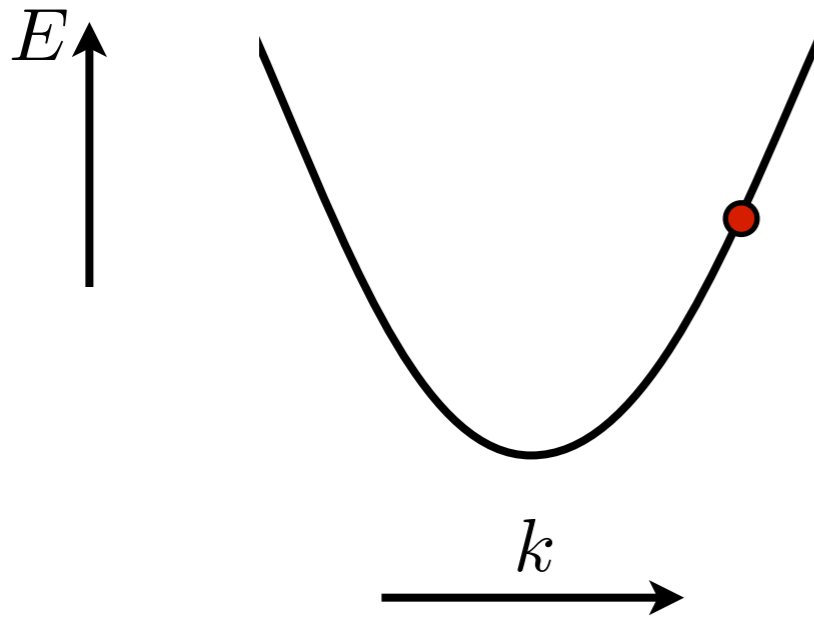
Anomalous plasmons

- (i) electron interactions + Berry curvature = new collective modes (“Berry Plasmons”)
- (ii) unusual Fermi-arc plasmons in Weyl semimetals

JS, Rudner, PNAS (2016)

JS, Rudner, arXiv (2017)

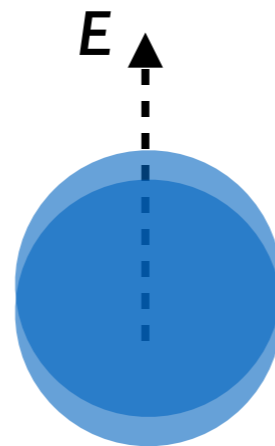
Solid state 101: “Vanilla” electrons



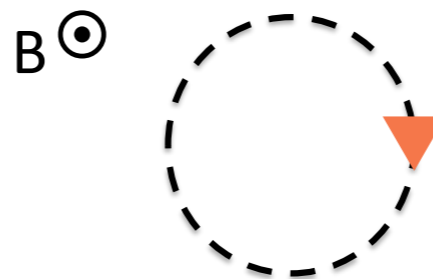
free-electron eq. of motion:

$$\dot{\mathbf{p}} = e\mathbf{v} \times \mathbf{B} + e\mathbf{E}$$

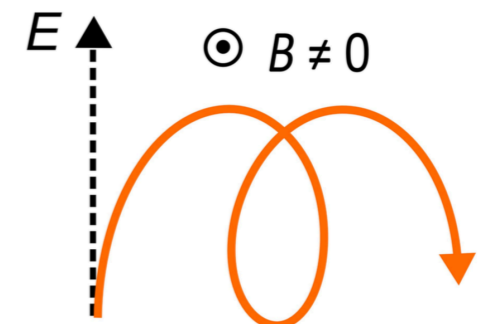
E pushes Fermi surface out of equilibrium



cyclotron motion



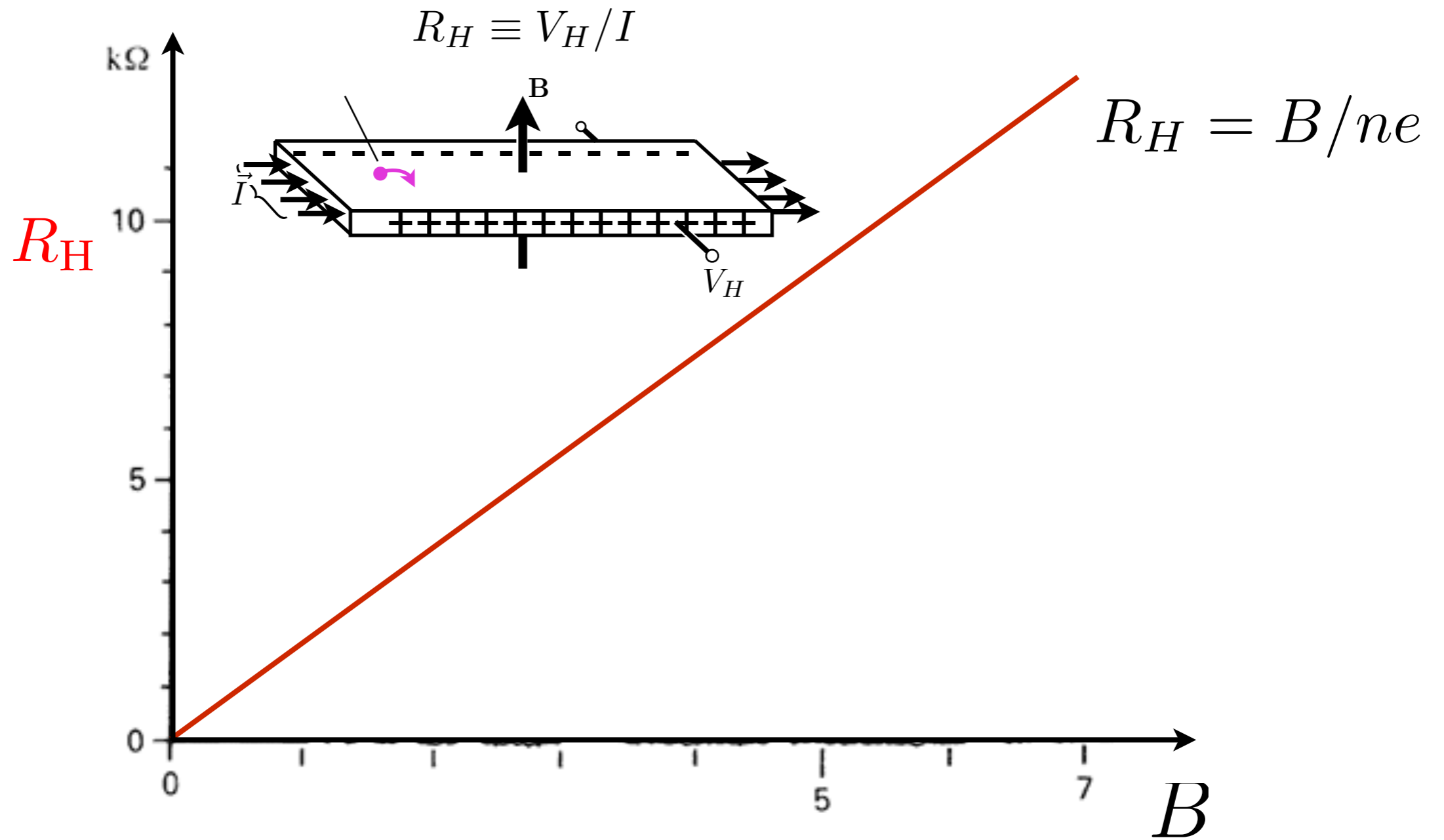
drifting cyclotron orbits



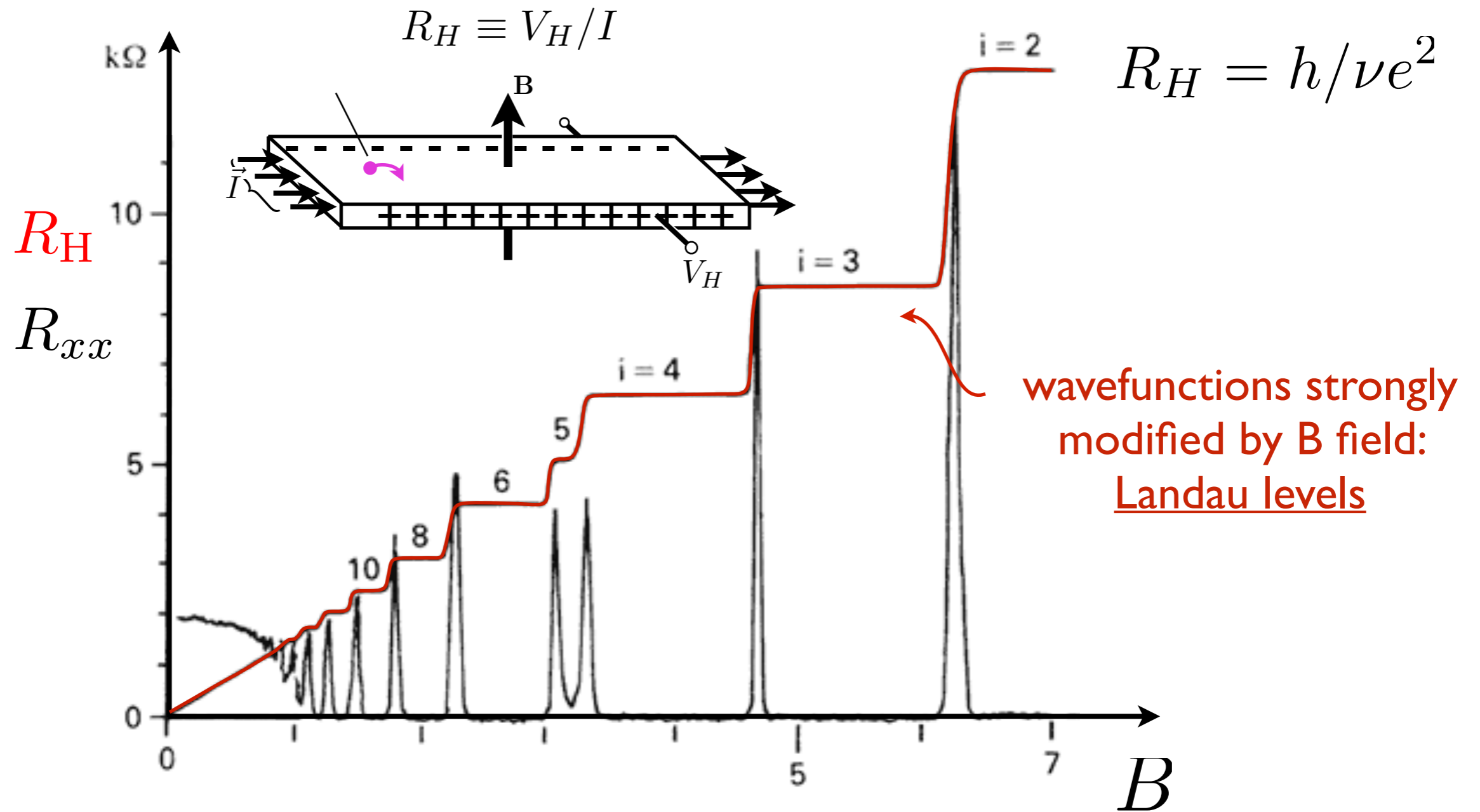
Litany of free electron properties:

- Fermi-surface + thermody. properties,
- Drude-type transport [e.g., electrical conductivity], and dynamical response
- Hall resistance,

Solid state IOI: Hall effect



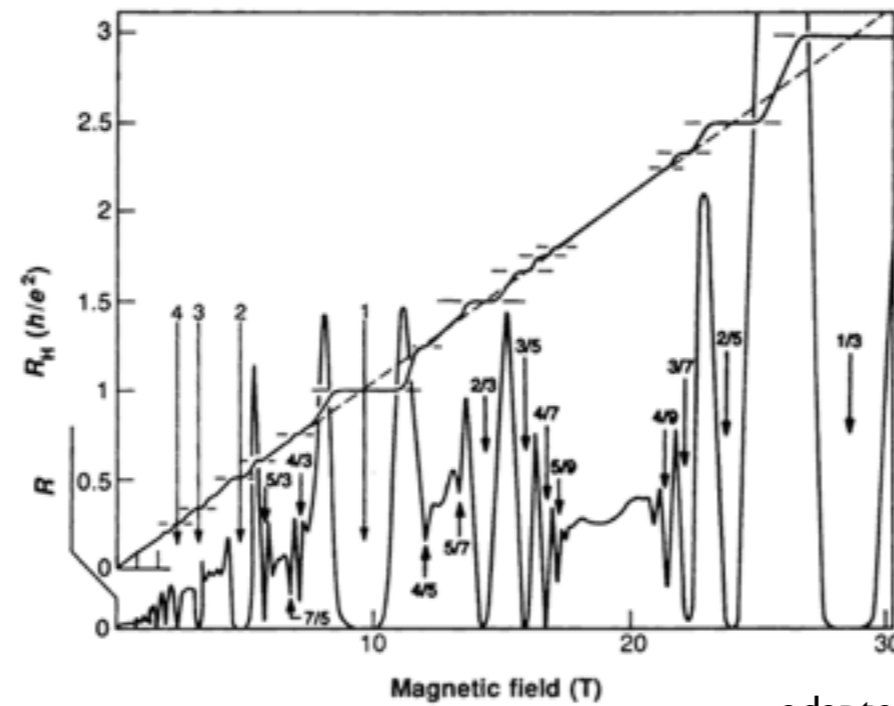
Quantum coloring: Quantum Hall effect



wavefunction matters: QH wavefunction gives *qualitatively* different behavior

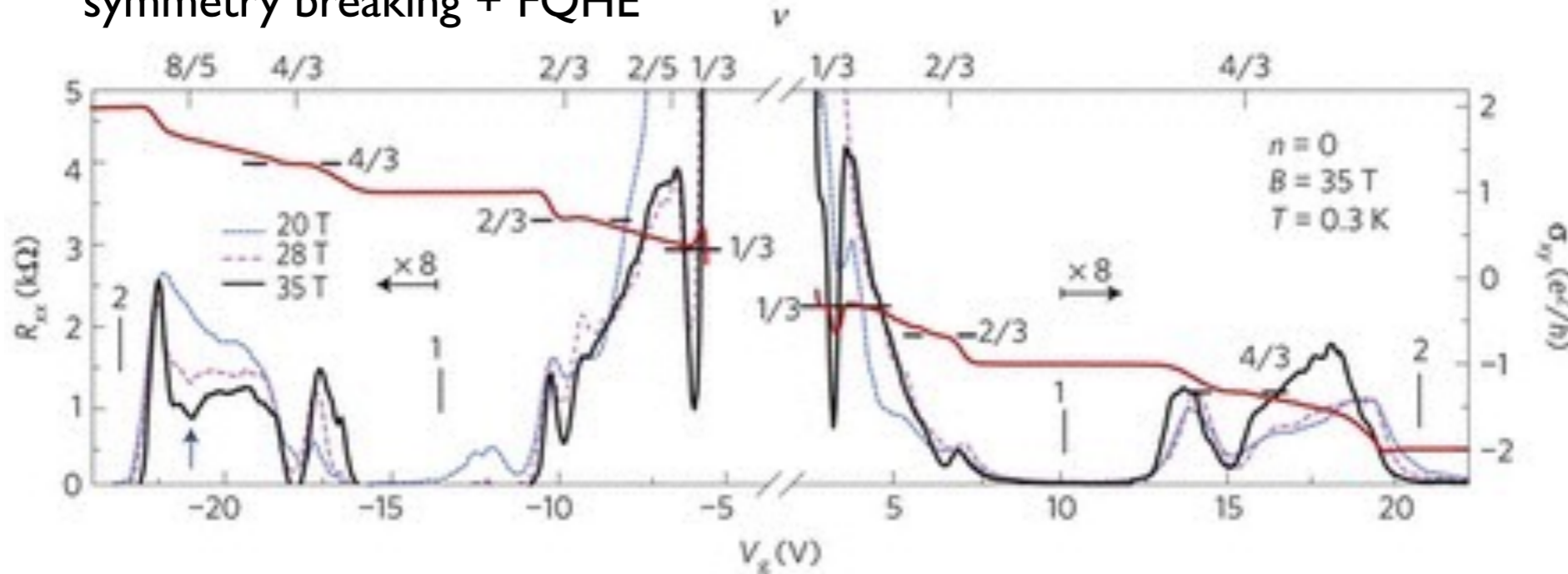
Quantum Hall systems possess rich phenomenology

fractional QHE



adapted from nobelprize.org

symmetry breaking + FQHE

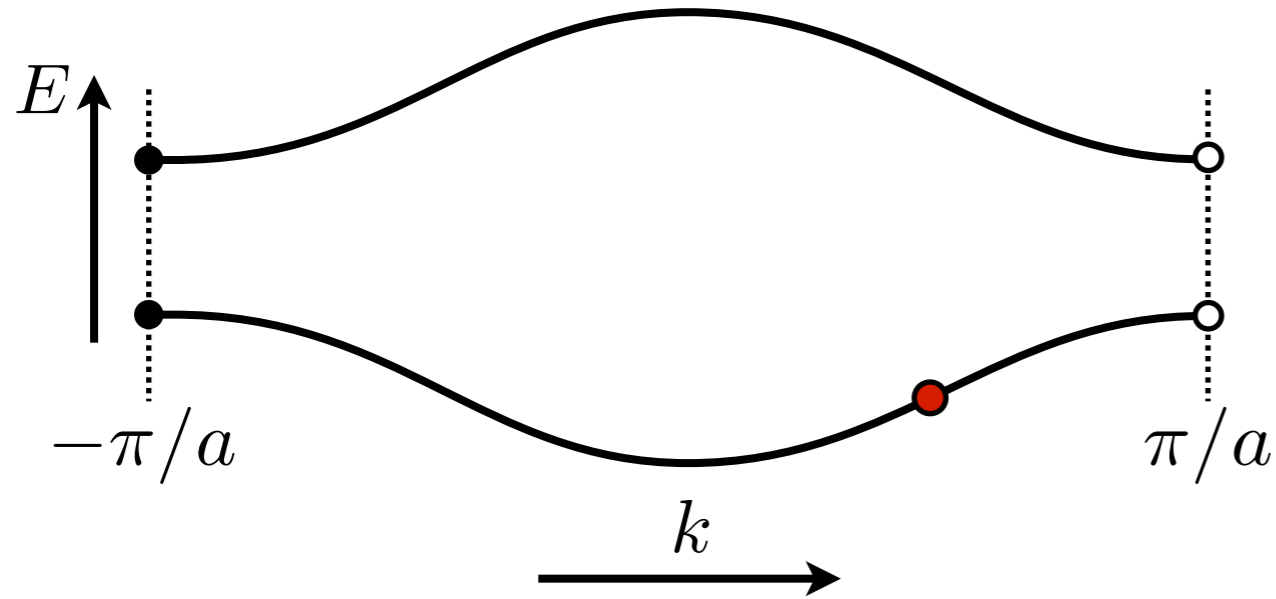


Kim and Shepard Groups, Nature Physics (2011), lots of others as well

Can we use crystal fields instead?

Quasiparticles in a crystal

Energy bands in a crystal; depends on k



Energy



Energy bands

Momentum



Quasi-momentum

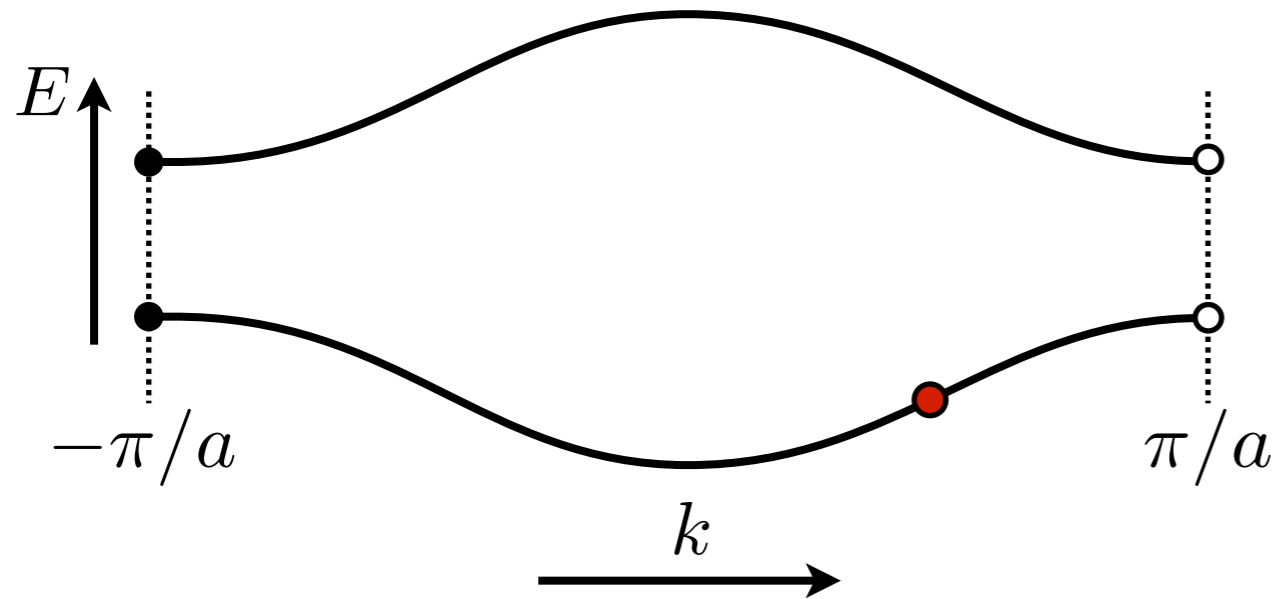
Mass



Effective mass

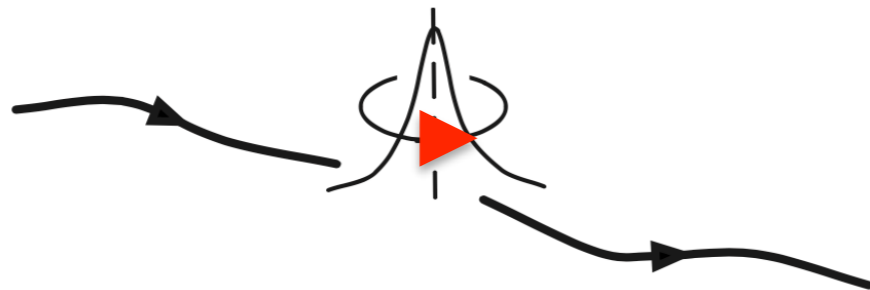
Wavefunction matters: **Berry curvature**

Energy bands in a crystal; depends on k



Energy	→	Energy bands
Momentum	→	Quasi-momentum
Mass	→	Effective mass

Emergent quantum mechanical property:

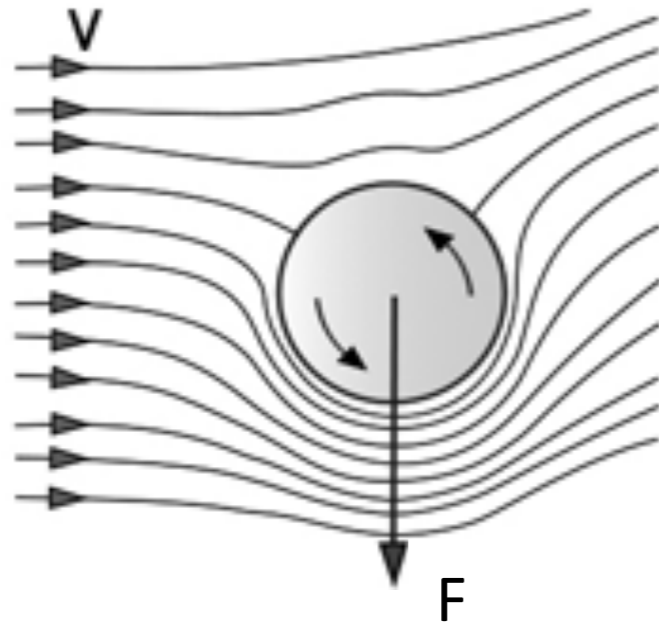


Berry curvature
(self-rotation of wavepackets)

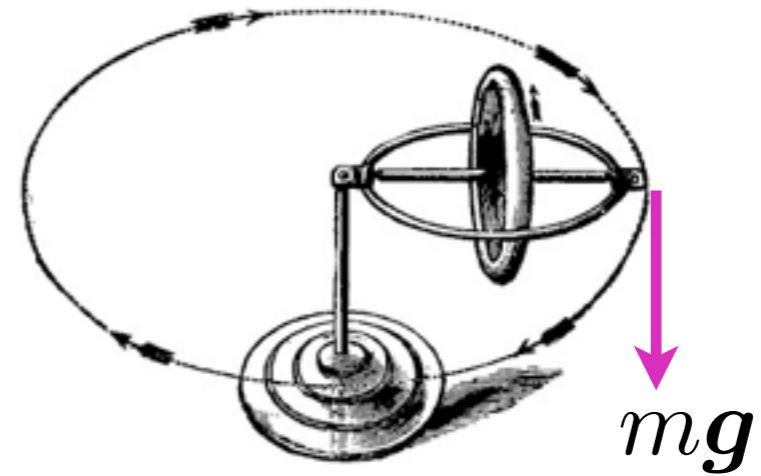
Electron wavepacket traveling through certain *special* crystals

(Self-) Rotation enables transverse motion

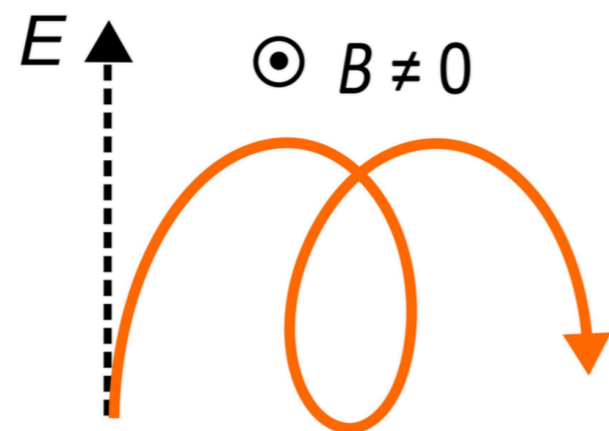
Magnus effect:



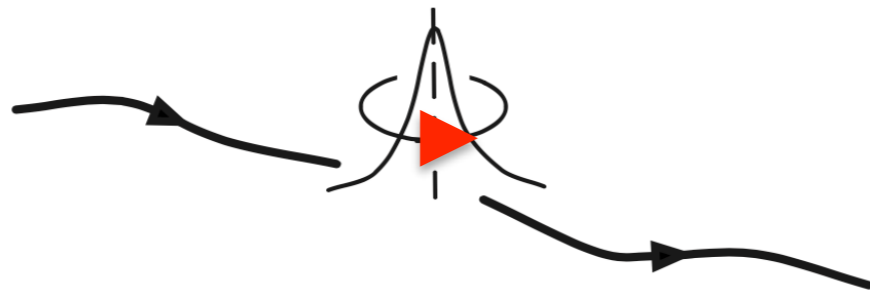
Gyroscopes:



Drifting cyclotron motion:



Anomalous velocity and Berry curvature $\Omega(\mathbf{p})$



Electron wavepacket traveling through certain *special* crystals

Contrasting trajectories

Semiclassical equations of motion

Group velocity

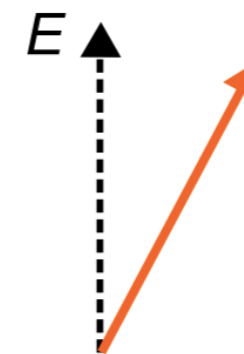
$$\dot{\mathbf{x}} = \frac{d\varepsilon}{d\mathbf{p}} + \dot{\mathbf{p}} \times \Omega$$

“Anomalous velocity”

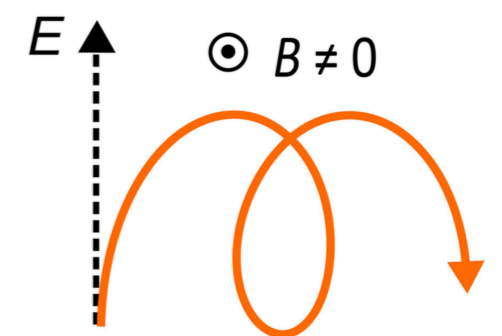
$$\dot{\mathbf{p}} = -\frac{dV}{d\mathbf{x}} + \dot{\mathbf{x}} \times \mathbf{B}$$

Lorentz force

Anomalous velocity:
Skewed trajectory:



Lorentz force:
Drifting cyclotron:



Zero-field quantum Hall effect

Model for a Quantum Hall Effect without Landau Levels: Condensed-Matter Realization of the “Parity Anomaly”

F. D. M. Haldane

Department of Physics, University of California, San Diego, La Jolla, California 92093

(Received 16 September 1987)

A two-dimensional condensed-matter lattice model is presented which exhibits a nonzero quantization of the Hall conductance σ^{xy} in the *absence* of an external magnetic field. Massless fermions *without spectral doubling* occur at critical values of the model parameters, and exhibit the so-called “parity anomaly” of (2+1)-dimensional field theories.

tight-binding “graphene” type model with complex second neighbor hopping

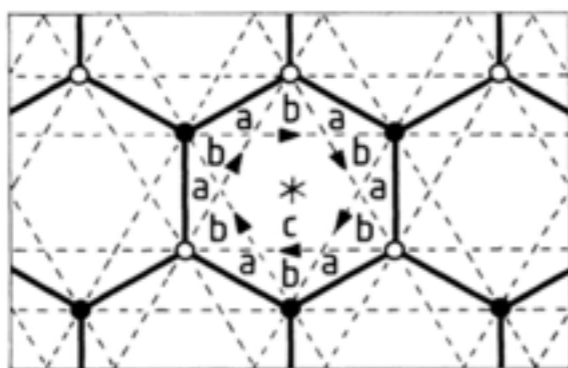


FIG. 1. The honeycomb-net model (“2D graphite”) showing nearest-neighbor bonds (solid lines) and second-neighbor bonds (dashed lines). Open and solid points, respectively, mark the *A* and *B* sublattice sites. The Wigner-Seitz unit cell is conveniently centered on the point of sixfold rotation symmetry (marked “*”) and is then bounded by the hexagon of nearest-neighbor bonds. Arrows on second-neighbor bonds mark the directions of positive phase hopping in the state with broken time-reversal invariance.

summing up Berry curvature over BZ

= topology

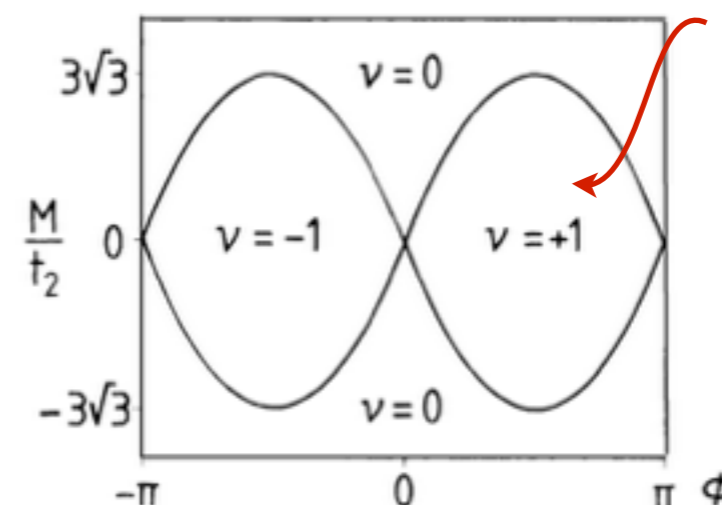
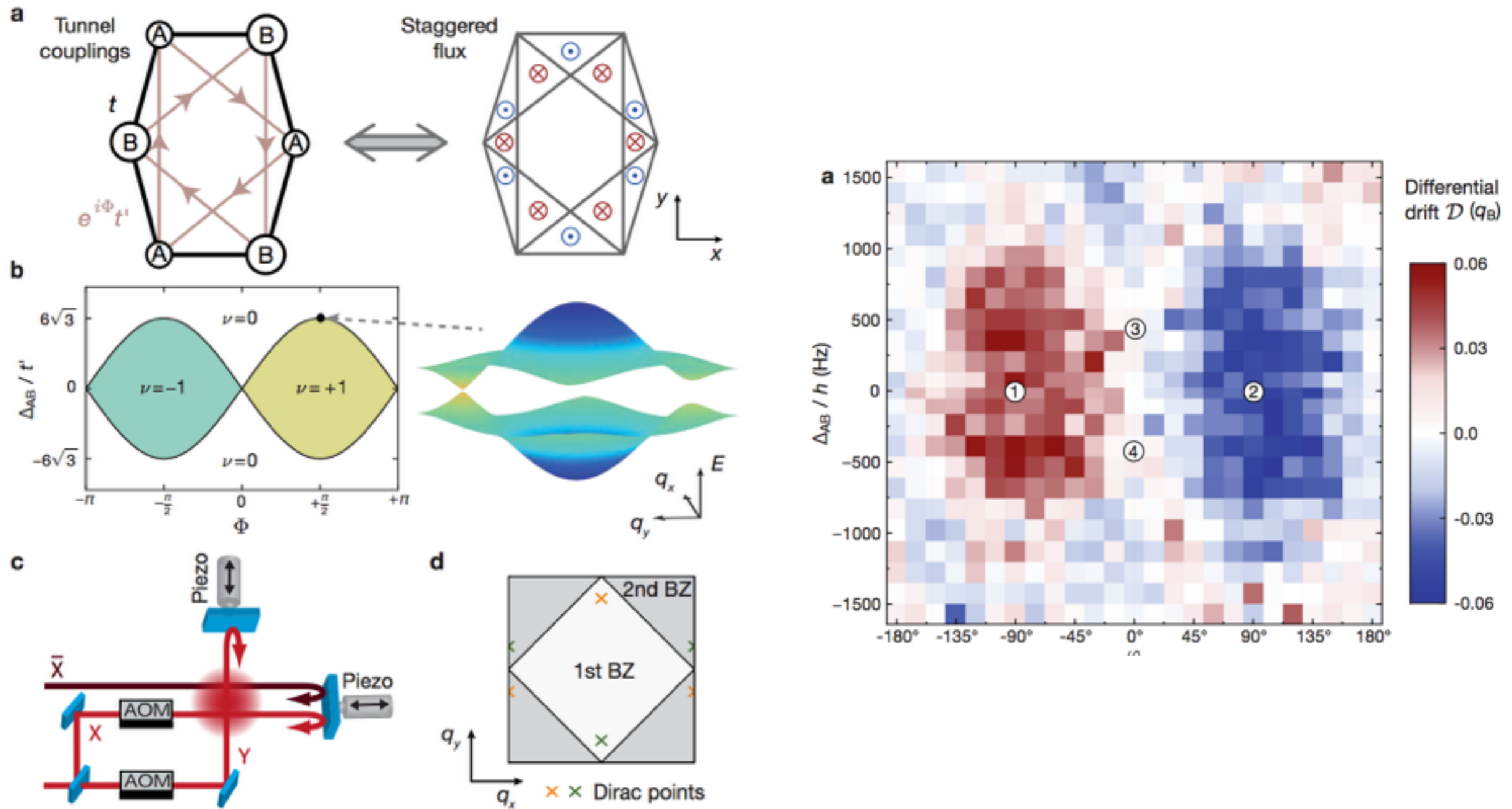


FIG. 2. Phase diagram of the spinless electron model with $|t_2/t_1| < \frac{1}{3}$. Zero-field quantum Hall effect phases ($\nu = \pm 1$, where $\sigma^{xy} = \nu e^2/h$) occur if $|M/t_2| < 3\sqrt{3}|\sin\phi|$. This figure assumes that t_2 is positive; if it is negative, ν changes sign. At the phase boundaries separating the anomalous and normal ($\nu=0$) semiconductor phases, the low-energy excitations of the model simulate undoubled massless chiral relativistic fermions.

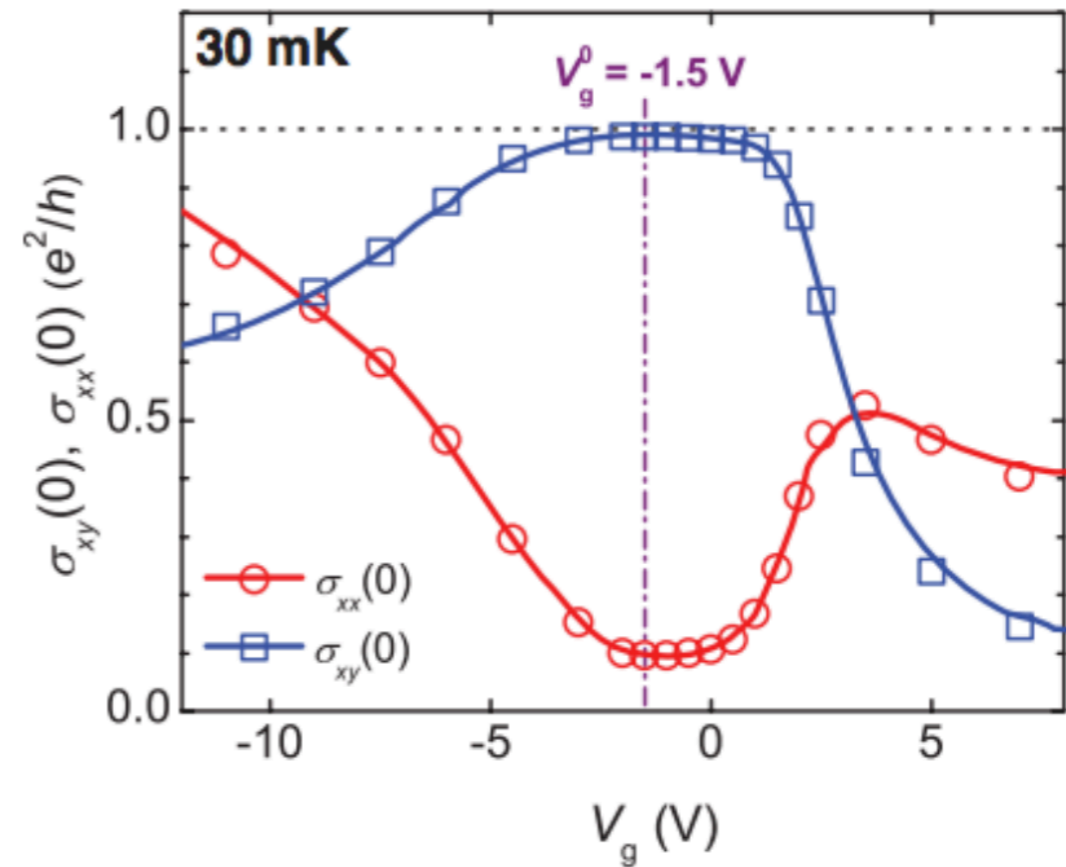
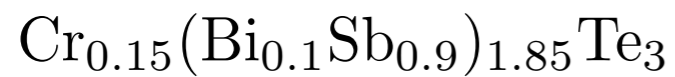
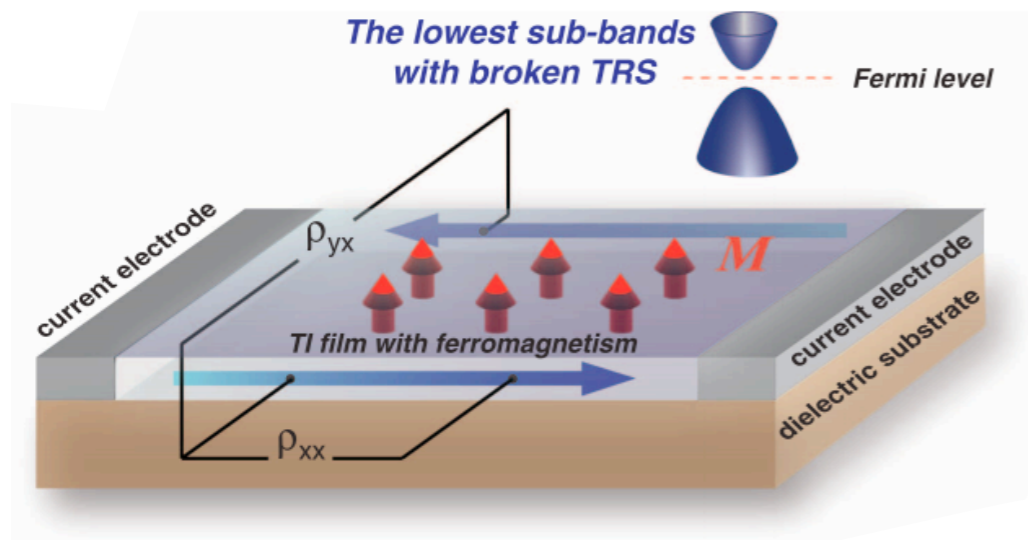
Realizing Haldane model and imaging Berry curvature



Electronic chirality without magnetic field

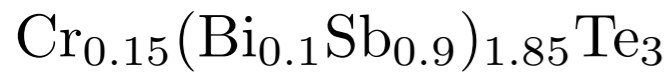
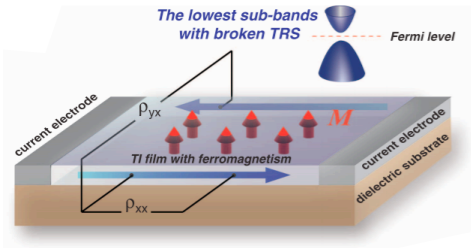
(Quantum) Anomalous Hall effect:

$$\mathbf{B} = 0$$



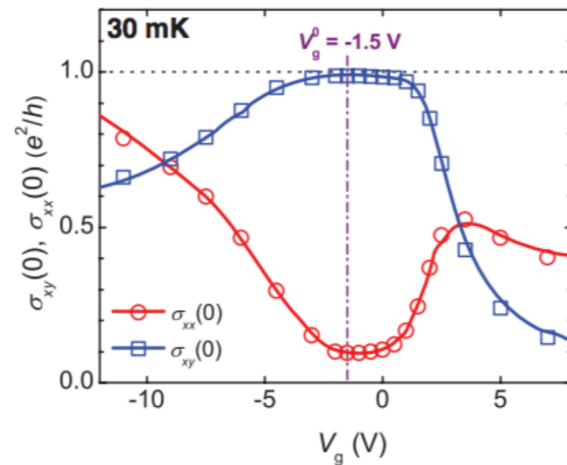
Topological materials: novel electronic + opto-electronics

(Quantum) Anomalous Hall effect:

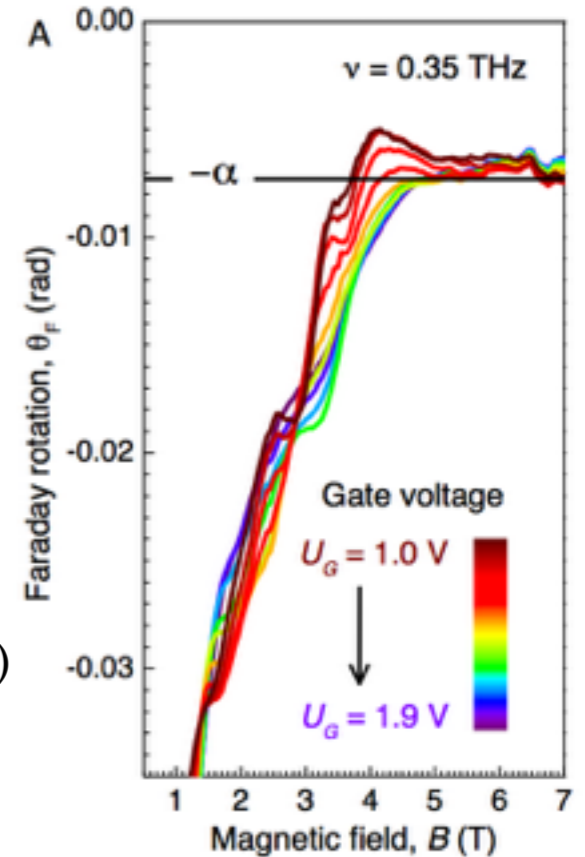
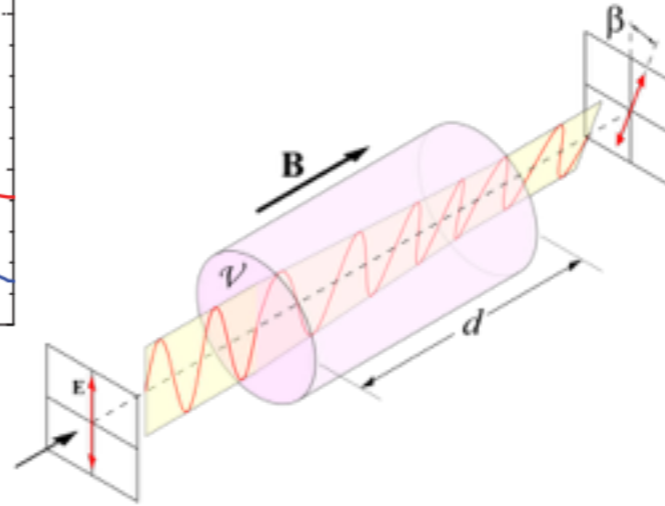


Zhang, et al, Science (2013)

$B = 0$



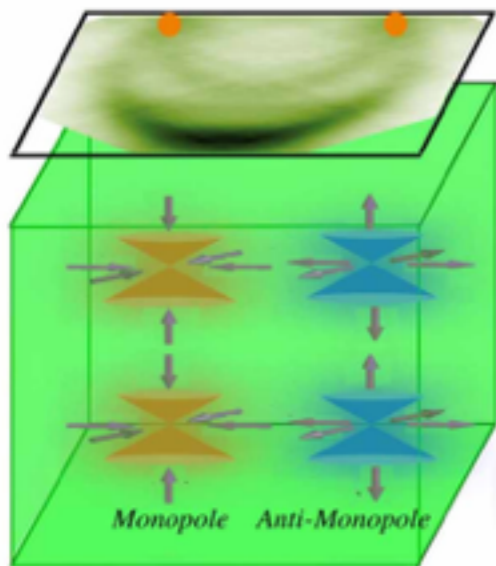
“Topological Magneto-electric effect” and
Quantized Faraday (and Kerr) rotations in 3D TIs



Strained HgTe 3D TI (Molenkamp group)
Dziom, et al, arXiv (2016)

see also
Bi₂Se₃ films, Wu et al (Armitage group), Science (2016)
& magnetic TI Okada, et al (Tokura group), Nat. Comm. (2016)

3D Weyl/Dirac semimetals & Fermi arcs

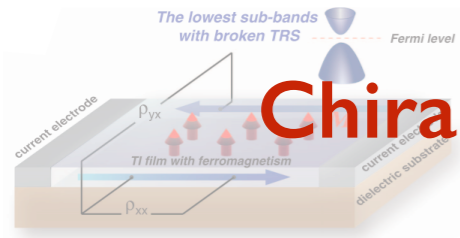


Weyl: TaAs,
Dirac: Cd₃As₂, Na₃Bi, ...

Xu et al, Science (2015), [Hasan group, and many others]

Topological materials: novel electronic + opto-electronics

(Quantum) Anomalous Hall effect

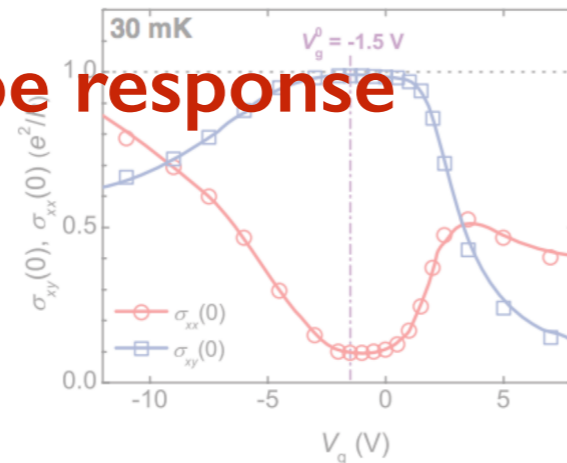


Chiral type response

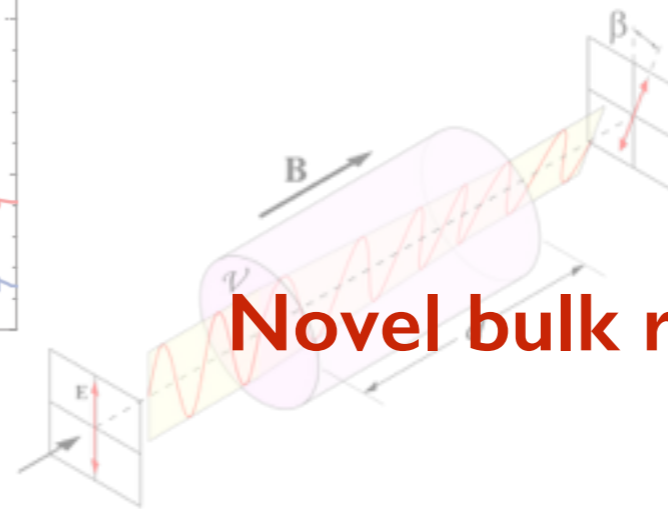


Zhang, et al, Science (2013)

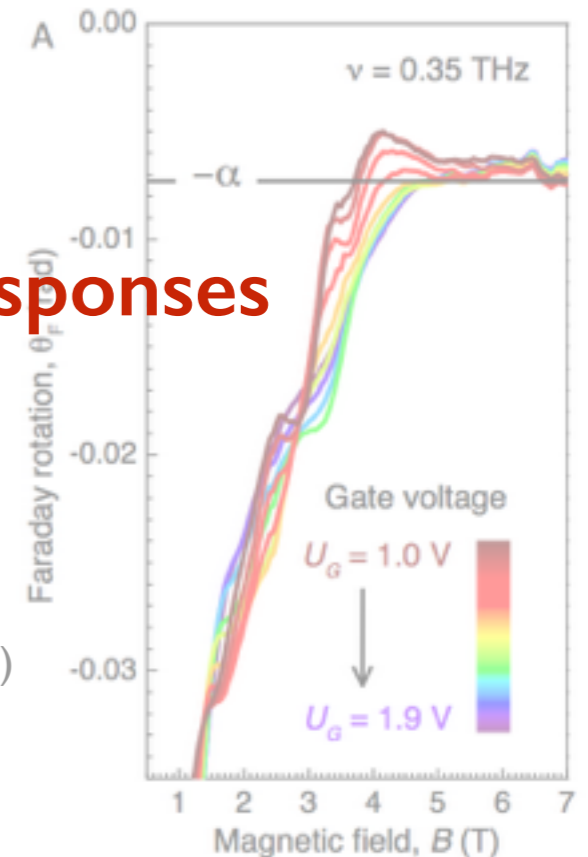
$B = 0$



“Topological Magneto-electric effect” and Quantized Faraday (and Kerr) rotations in 3D TIs



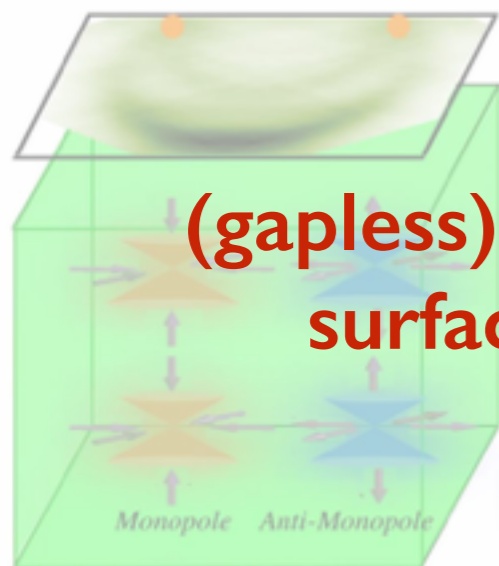
Novel bulk responses



Strained HgTe 3D TI (Molenkamp group)
Dziom, et al, arXiv (2016)

see also
Bi₂Se₃ films, Wu et al (Armitage group), Science (2016)
& magnetic TI Okada, et al (Tokura group), Nat. Comm.

3D Weyl/Dirac semimetals & Fermi arcs



(gapless) topological surface states

Weyl: TaAs, Dirac: Cd₃As₂, Na₃Bi, ...

Xu et al, Science (2015), [Hasan group, and many others]

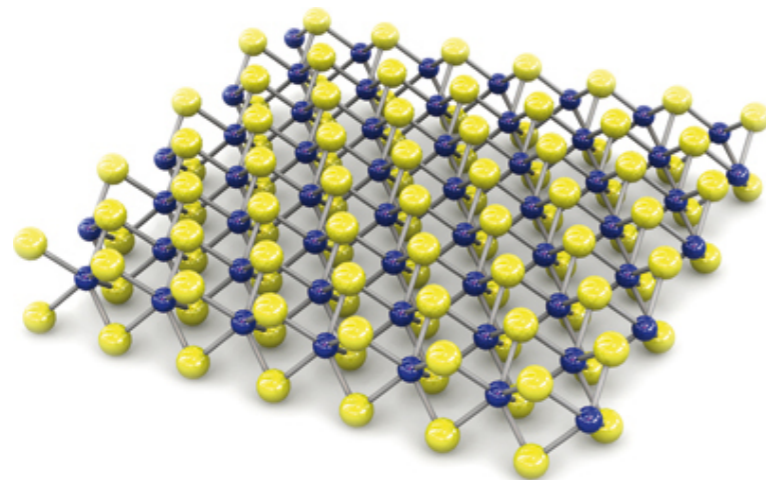
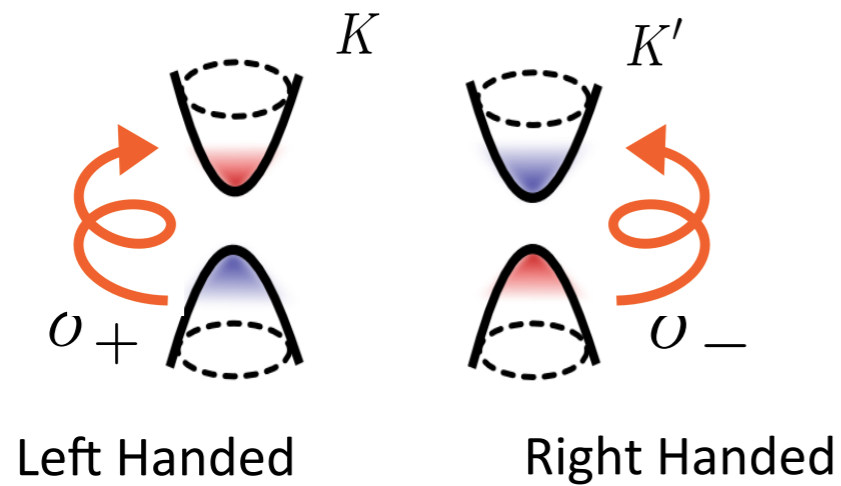
Hall regime: Transverse motion dominates response

$$\sigma_{xy} \gg \sigma_{xx}$$

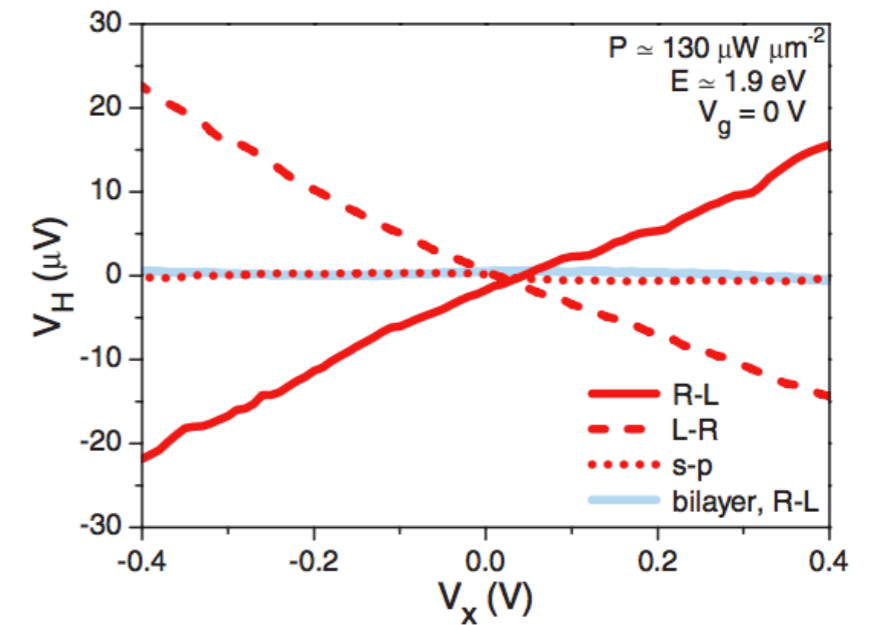
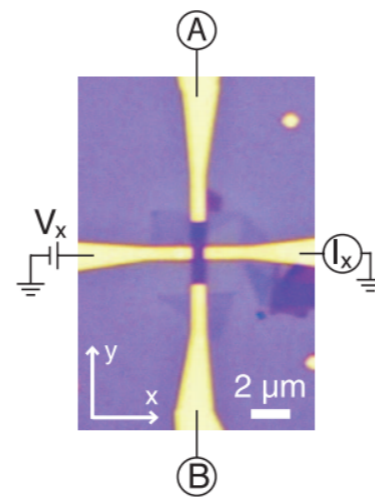
Search for new “topological” flavored responses in more readily available materials?

Hall photoconductivity in gapped Dirac materials

Circularly polarized light absorption in MoS₂



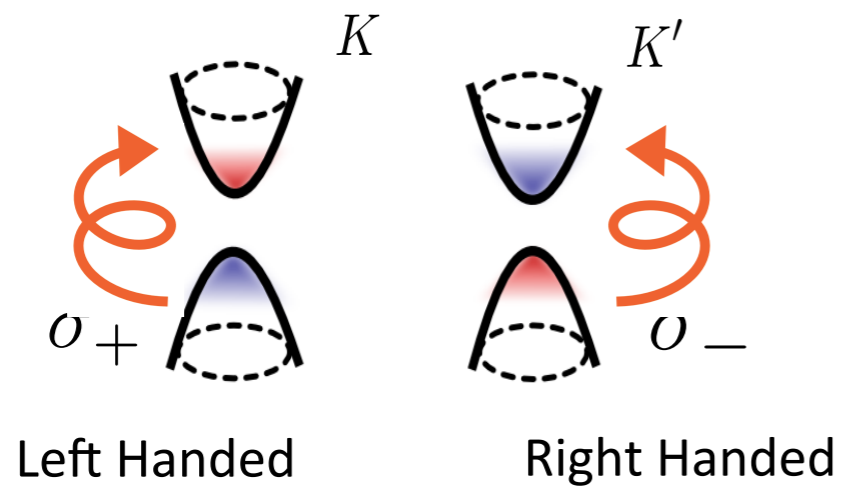
Hall effect at zero magnetic field



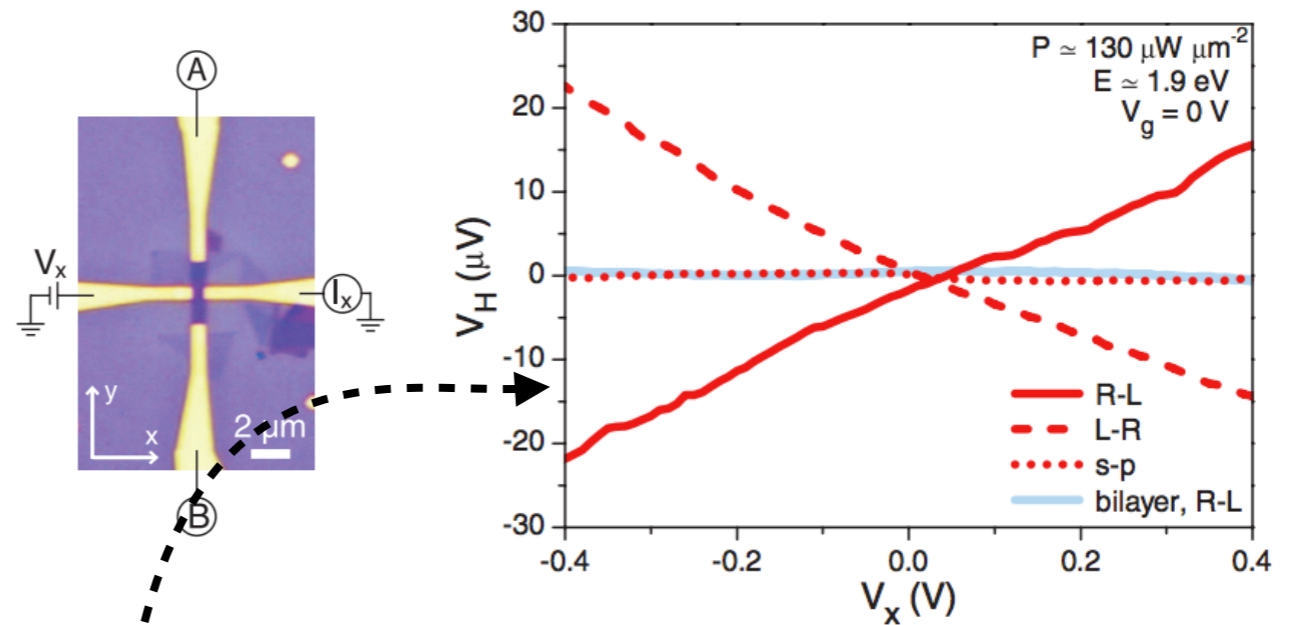
KF Mak, K McGill, JW Park, PL McEuen, Science (2014)

Hall photoconductivity in gapped Dirac materials

Circularly polarized light absorption in MoS₂



Hall effect at zero magnetic field



KF Mak, K McGill, JW Park, PL McEuen, Science (2014)

Effect is tiny

Hall photoconductivity:

$$\begin{aligned} \sigma_{xy} &\sim 1 \text{ nS} \\ &= 2.5 \times 10^{-5} [e^2/h] \end{aligned}$$

$$\sigma_{xx} \gg \sigma_{xy}$$

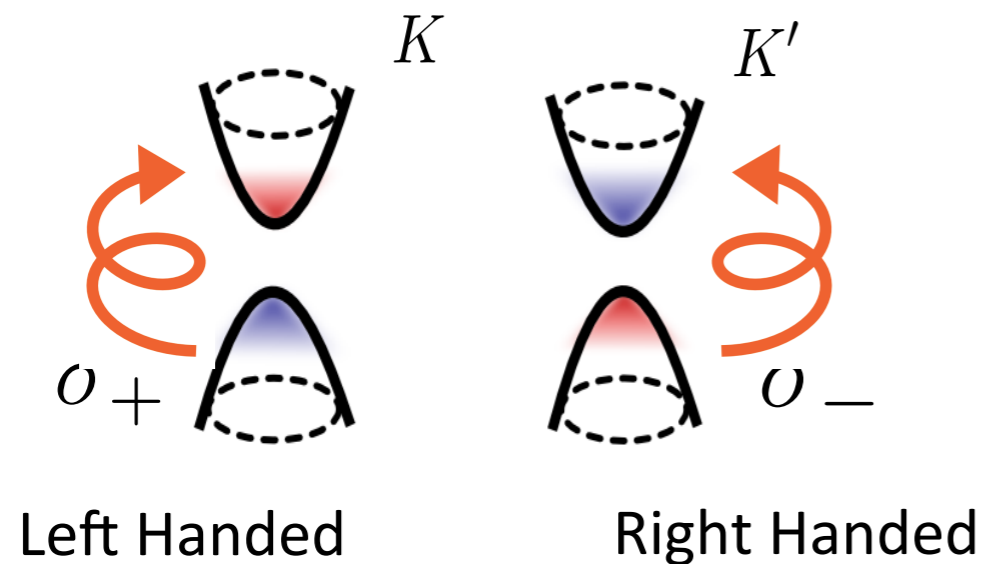
Can we achieve Hall regime in gapped Dirac materials?

Plan

Part I.

Giant Hall photoconductivity

gapped Dirac materials with a narrow gap yield Hall photoconductivity order $\sim e^2/h$; access to “Berry” transport regime



JS, Kats, Nano Letters (2016)

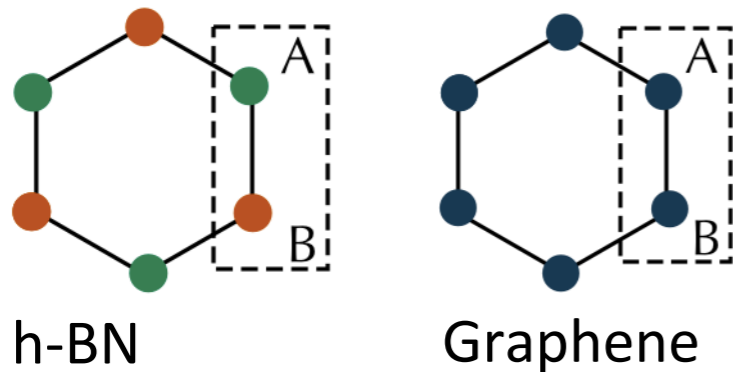
In collaboration with:



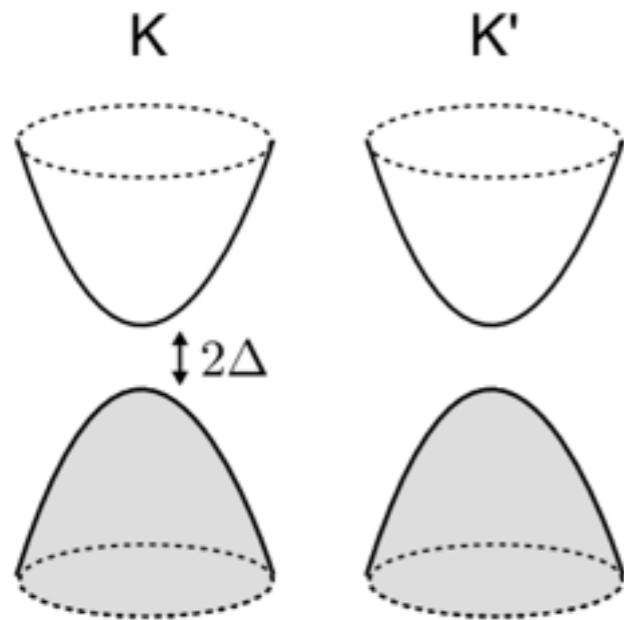
Mikhail Kats
(Wisconsin)

Narrow gapped Dirac materials (GDM)

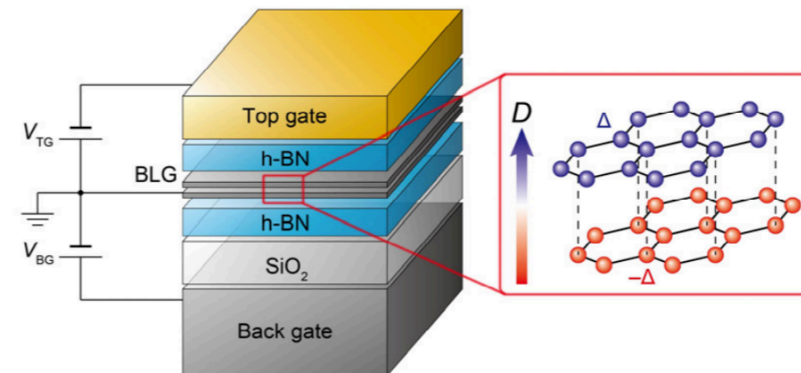
G/h-BN heterostructures



narrow gaps: $\Delta \approx 5 - 30 \text{ meV}$

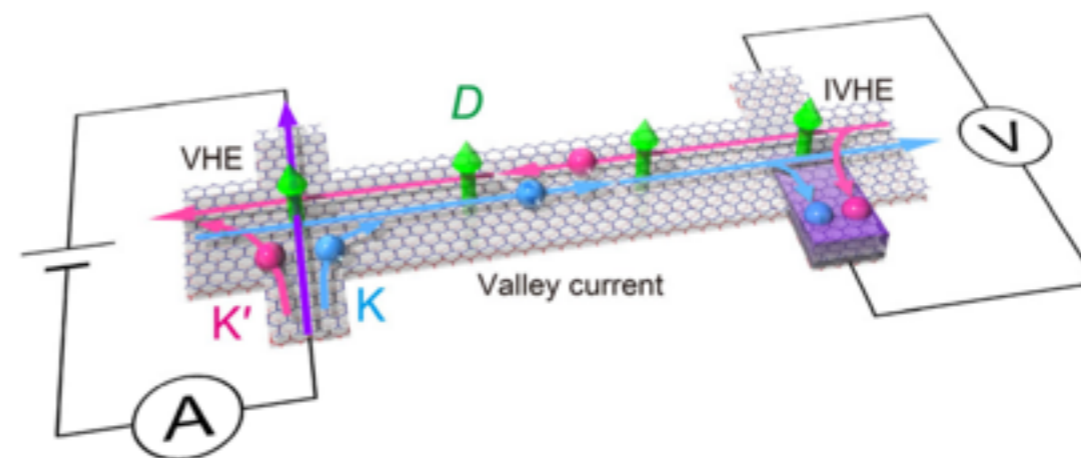


Dual-gated Bilayer graphene



Tunable gaps from 0 up to 100-200 meV

Berry curvature and Valley Hall effect observed



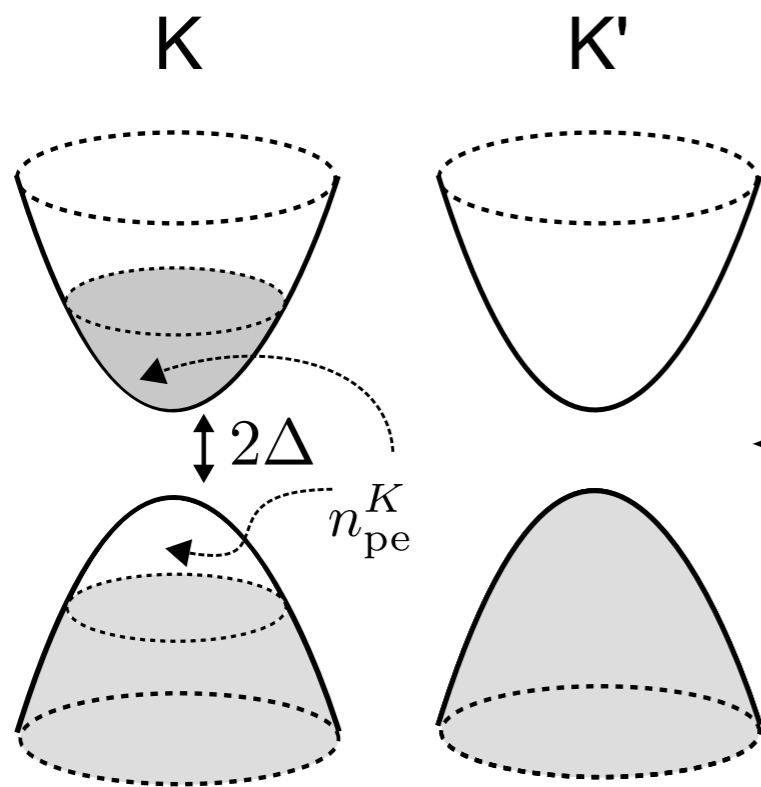
G/hBN: Gorbachev, JS, et al, Science (2014),

Dual-gated bilayer graphene: Shimazaki, et al Nature Physics (2015), Sui, et al Nature Physics (2015)

Giant Hall photoconductivity in narrow gap GDMs

Intrinsic Hall photoconductivity:

$$\sigma_{xy} = \frac{Ne^2}{\hbar} \left[\sum_{\mathbf{p}, \pm} f_{\pm}^K(\mathbf{p}) \Omega_{\pm}^K(\mathbf{p}) + \sum_{\mathbf{p}, \pm} f_{\pm}^{K'}(\mathbf{p}) \Omega_{\pm}^{K'}(\mathbf{p}) \right]$$



photoexcited carrier density

For gapped Dirac materials (GDMs):

$$\sigma_{xy}^{\text{pe}} = \frac{Ne^2}{h} \left[\mathcal{F}_K(n_{\text{pe}}^K/2) + \mathcal{F}_{K'}(n_{\text{pe}}^{K'}/2) \right],$$

$$\mathcal{F}_{\zeta}(x) = \frac{\zeta}{2} \left(1 - \left[\frac{\tilde{n}^{1/2}}{\sqrt{\tilde{n} + n_0 + x}} + \frac{\tilde{n}^{1/2}}{\sqrt{\tilde{n} + x}} \right] \right),$$

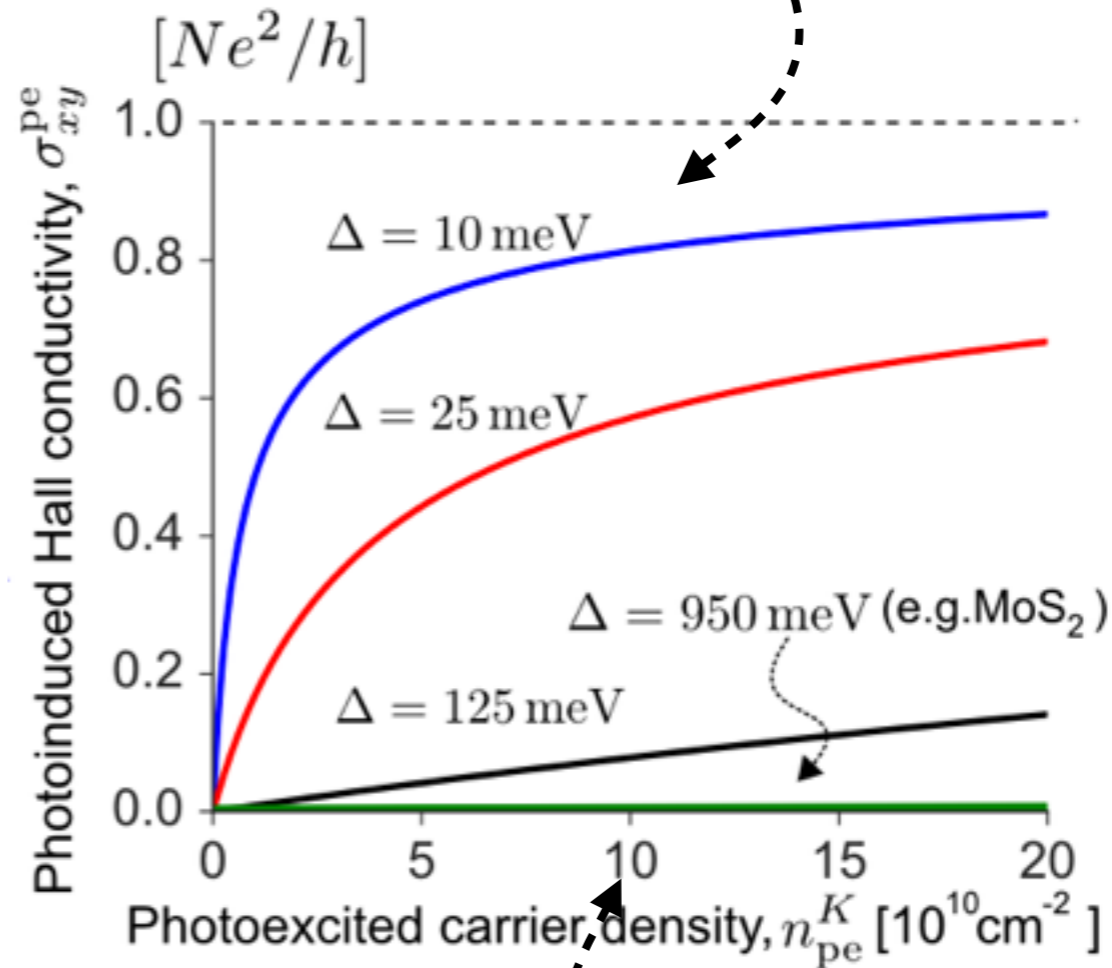
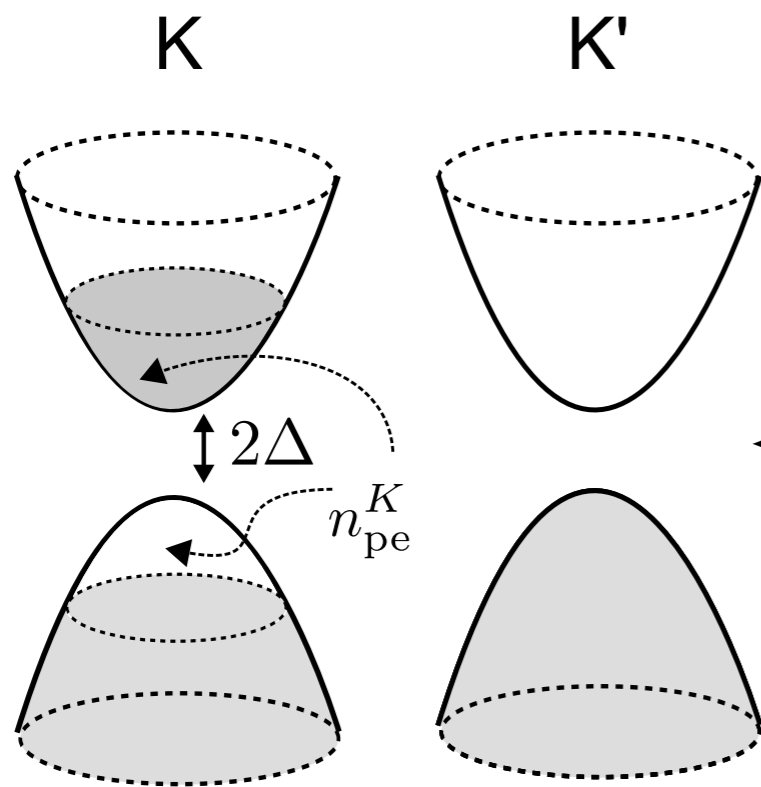
dependent on gap size

$$\tilde{n} = \Delta^2 / 4\pi v^2 \hbar^2$$

+1(-1) for K (K')

Giant Hall photoconductivity in narrow gap GDMs

(i) narrow gaps yield giant $\sigma_{xy} \sim e^2/h$

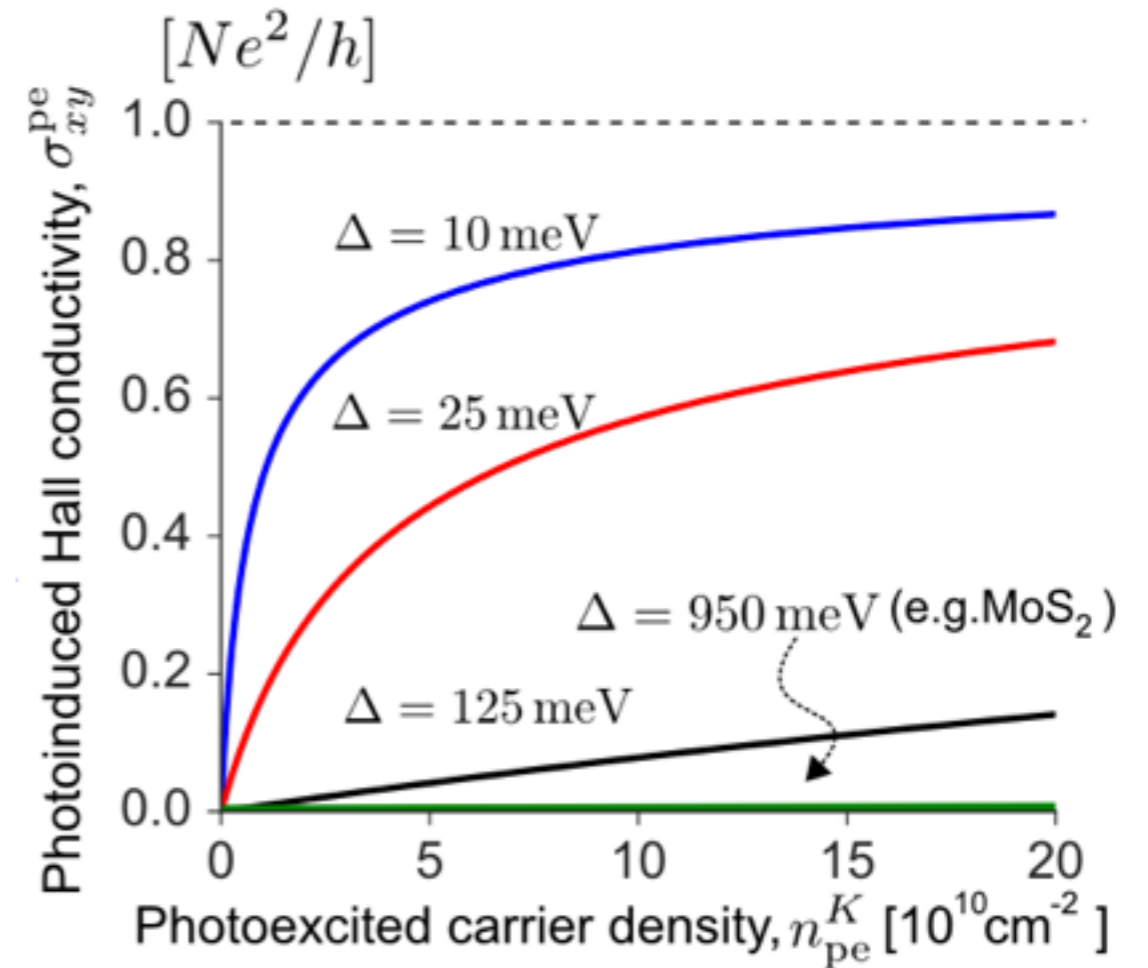
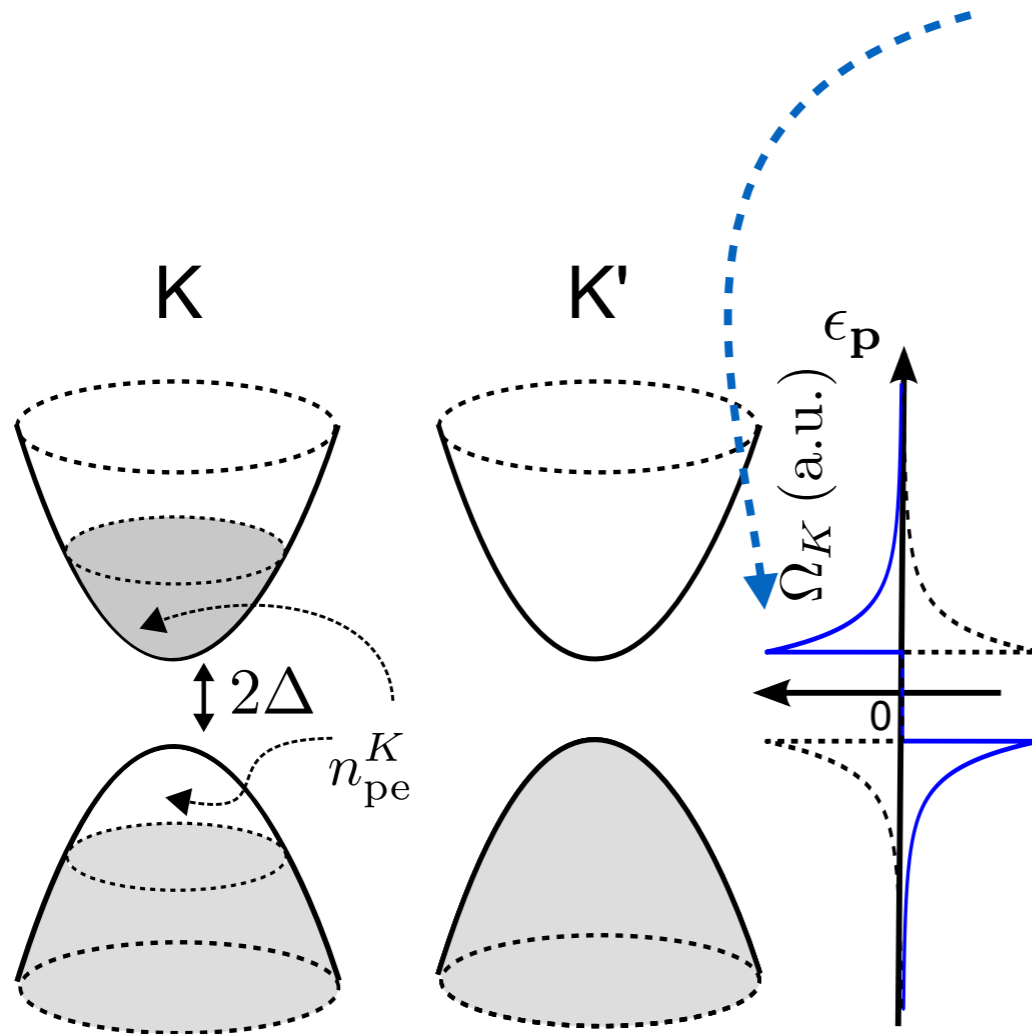


(iii) giant change, several orders of magnitude

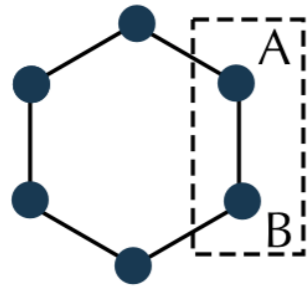
(ii) achievable even for small $n_{pe}^K \sim 10^{10} \text{cm}^{-2}$

Giant Hall photoconductivity in narrow gap GDMs

Berry curvature and Anomalous velocity concentrated at band extrema



Intuitive explanation: pseudo-spin and velocity

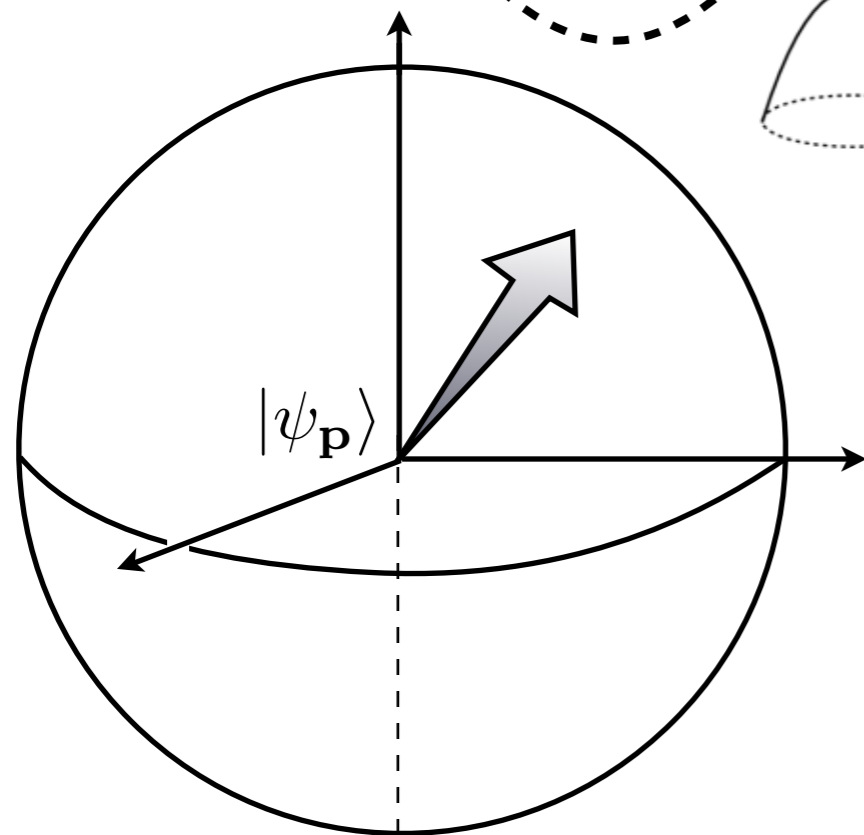
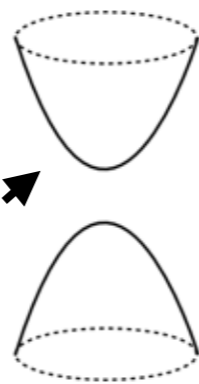


velocity depends on amplitude + phase on A/B sub lattice

e.g. at band extrema, velocity vanishes (all on A site)

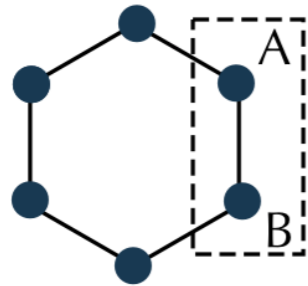
$$\mathbf{v}_{\mathbf{p}} = \langle \psi(\mathbf{p}) | \boldsymbol{\sigma} | \psi(\mathbf{p}) \rangle$$

all on A site



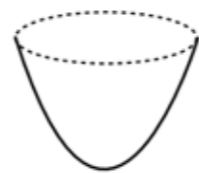
all on B site

Intuitive explanation: pseudo-spin and velocity



velocity depends on amplitude + phase on A/B sub lattice

all on A site

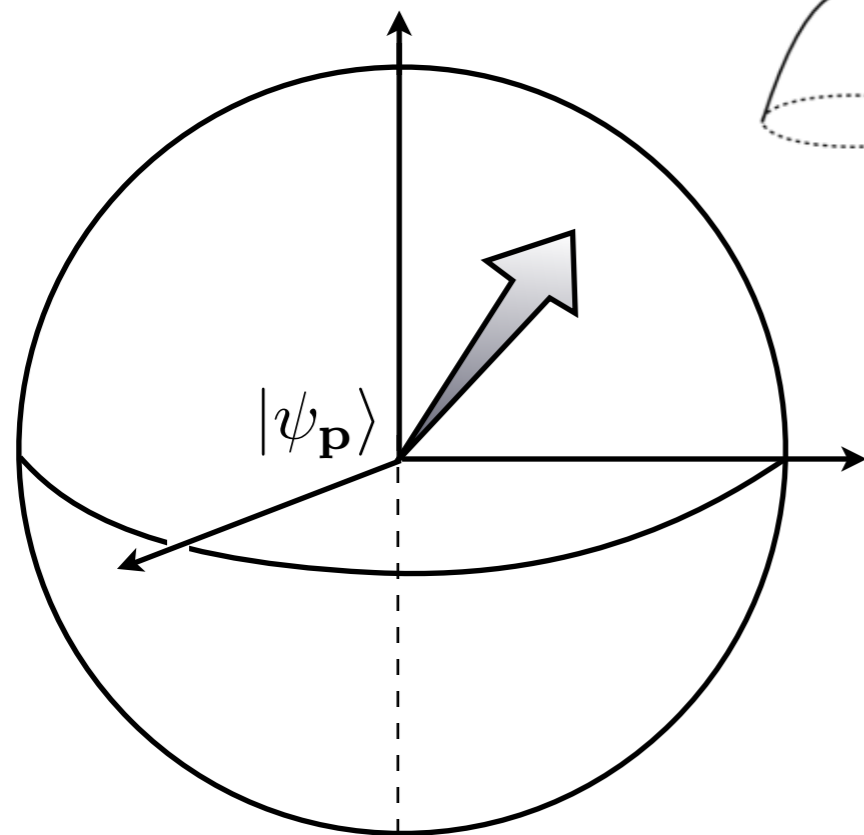


$$\mathbf{v}_{\mathbf{p}} = \langle \psi(\mathbf{p}) | \boldsymbol{\sigma} | \psi(\mathbf{p}) \rangle$$

Apply electric field, wave function is perturbed

$$|\psi_{-}(\mathbf{p})\rangle = \psi_{-}^{(0)}(\mathbf{p}) + \frac{\langle \psi_{+}^{(0)} | H' | \psi_{-}^{(0)} \rangle}{\epsilon_{-}(\mathbf{p}) - \epsilon_{+}(\mathbf{p})} |\psi_{+}^{(0)}\rangle$$

↖ perturbation



all on B site



anomalous equation of motion

$$\dot{\mathbf{x}} = \frac{d\epsilon}{d\mathbf{p}} + \dot{\mathbf{p}} \times \boldsymbol{\Omega}$$

↖ 1st order perturbation theory

JS, Kats, Nano Letters (2016)

Enhancement of valley imbalance rate

Fermi's golden rule (valley selective absorption rate)

$$W_{K(K')} = \frac{2\pi}{\hbar} \sum_{\mathbf{k}} |M_{\mathbf{k}}^{K(K')}|^2 \delta(\epsilon_{\mathbf{k}} - \hbar\omega/2)$$

Valley population imbalance rate:

$$\frac{d\delta n}{dt} = 2(W_K^d - W_{K'}^d) = d \frac{e^2 |\mathbf{E}|^2}{\hbar^2 \omega} \frac{\Delta}{\hbar\omega}$$

maximized when $\hbar\omega = 2\Delta$

Hall photoconductivity per fluence:

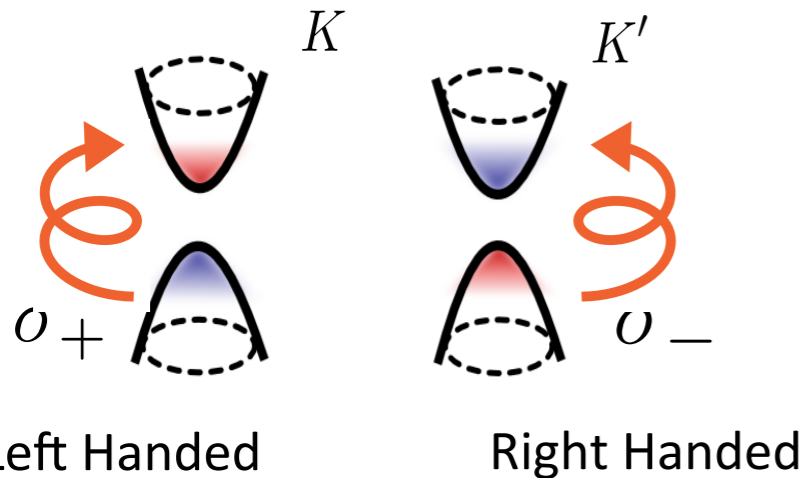
$$\frac{\tilde{\sigma}_{xy}^{\text{pe}}}{\mathcal{P}_{\text{in}}} = d \frac{S_0}{(\hbar\omega)^2 \Delta},$$

characteristic conductivity per fluence

scales as $\propto \Delta^{-3}$ on resonance

six orders of magnitude enhancement for

$$\Delta = 1 \text{ eV} \rightarrow 10 \text{ meV}$$



How large? Accessing Hall regime $\sigma_{xy} \gg \sigma_{xx}$

$$\tan \theta_H = \sigma_{xy}^{\text{pe}} / \sigma_{xx}^{\text{pe}}$$

longitudinal motion:

$$\sigma_{xx}^{\text{pe}} = eN\eta n_{\text{pe}}$$

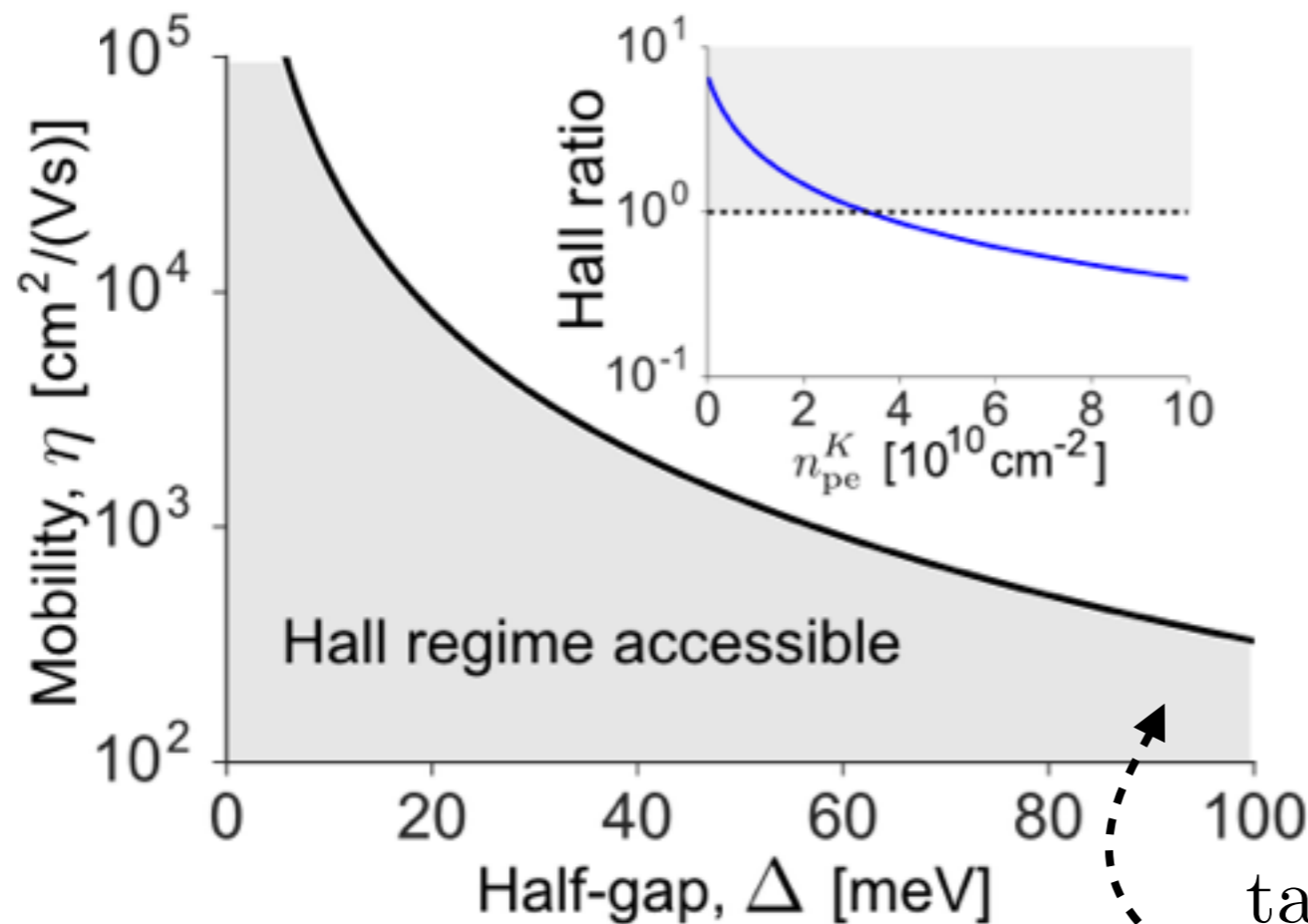
mobility

transverse motion:

$$\sigma_{xy}^{\text{pe}} = \frac{Ne^2}{h} \left[\mathcal{F}_K(n_{\text{pe}}^K/2) + \mathcal{F}_{K'}(n_{\text{pe}}^{K'}/2) \right],$$

$$\mathcal{F}_\zeta(x) = \frac{\zeta}{2} \left(1 - \left[\frac{\tilde{n}^{1/2}}{\sqrt{\tilde{n} + n_0 + x}} + \frac{\tilde{n}^{1/2}}{\sqrt{\tilde{n} + x}} \right] \right),$$

dependent on gap size



$$\tan \theta_H > 1$$

**Hall (transverse) motion
overwhelms longitudinal motion**

Signatures of the Hall regime: $\sigma_{xy} \gg \sigma_{xx}$

Magneto-transport: Lorentz force
impedes longitudinal motion

$$\dot{\mathbf{x}} = \frac{d\epsilon}{d\mathbf{p}}$$

$$\dot{\mathbf{p}} = -\frac{dV}{d\mathbf{x}} + \dot{\mathbf{x}} \times \mathbf{B}$$

Signatures of the “Berry” Hall regime: $\sigma_{xy} \gg \sigma_{xx}$

Magneto-transport: Lorentz force
impedes longitudinal motion

$$\dot{\mathbf{x}} = \frac{d\epsilon}{d\mathbf{p}}$$

$$\dot{\mathbf{p}} = -\frac{dV}{d\mathbf{x}} + \dot{\mathbf{x}} \times \mathbf{B}$$

“Berry transport”: Berry curvature
boosts longitudinal motion

$$\dot{\mathbf{x}} = \frac{d\epsilon}{d\mathbf{p}} + \dot{\mathbf{p}} \times \Omega$$

$$\dot{\mathbf{p}} = -\frac{dV}{d\mathbf{x}}$$

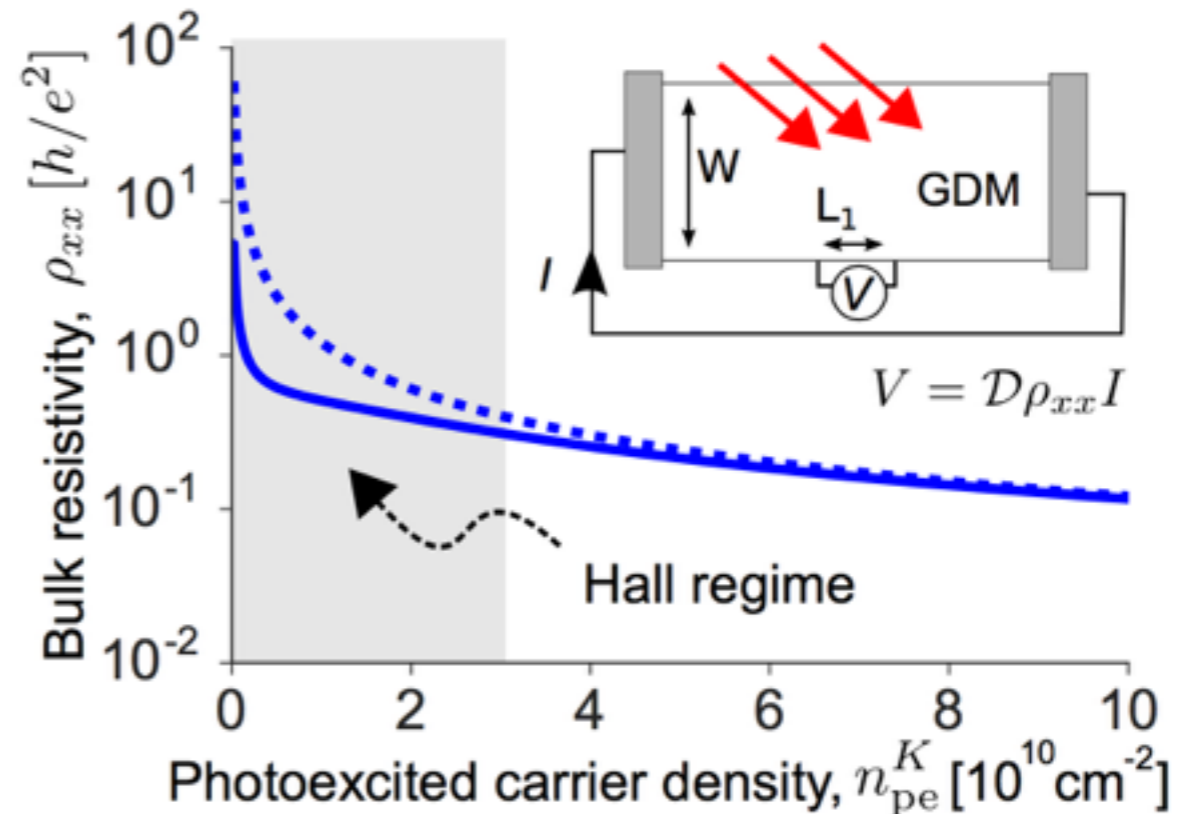
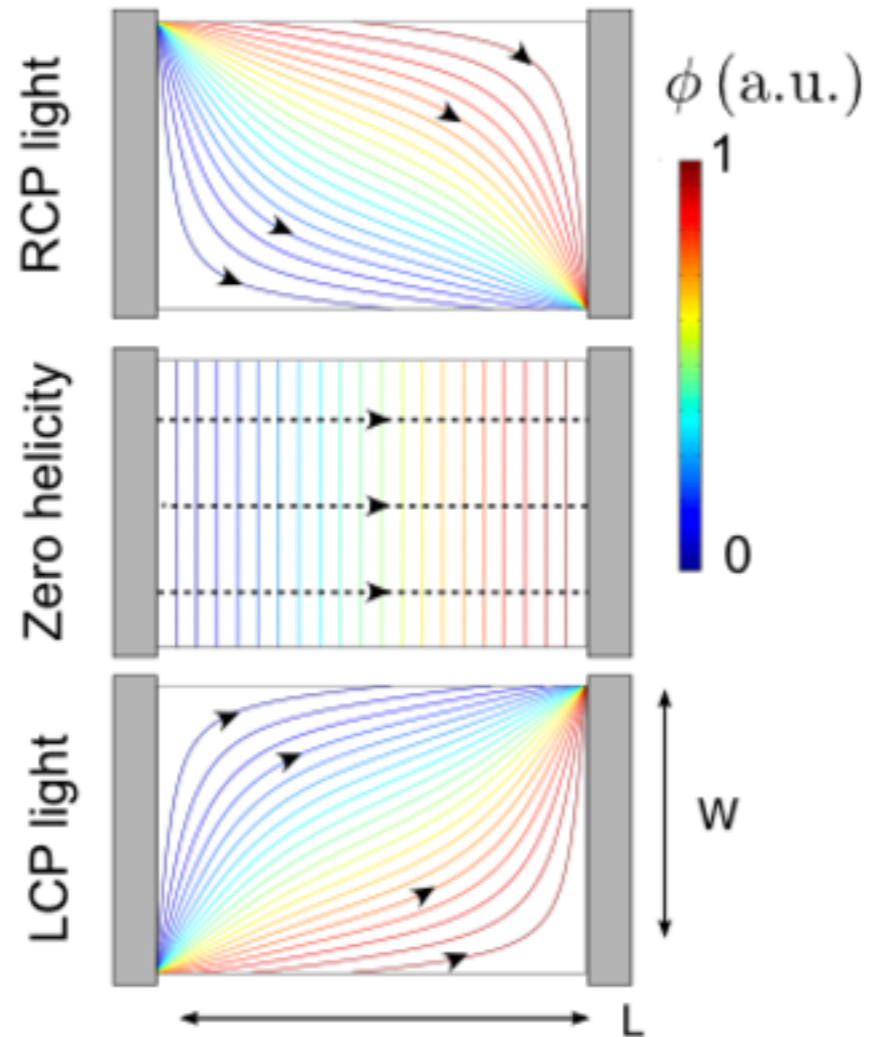
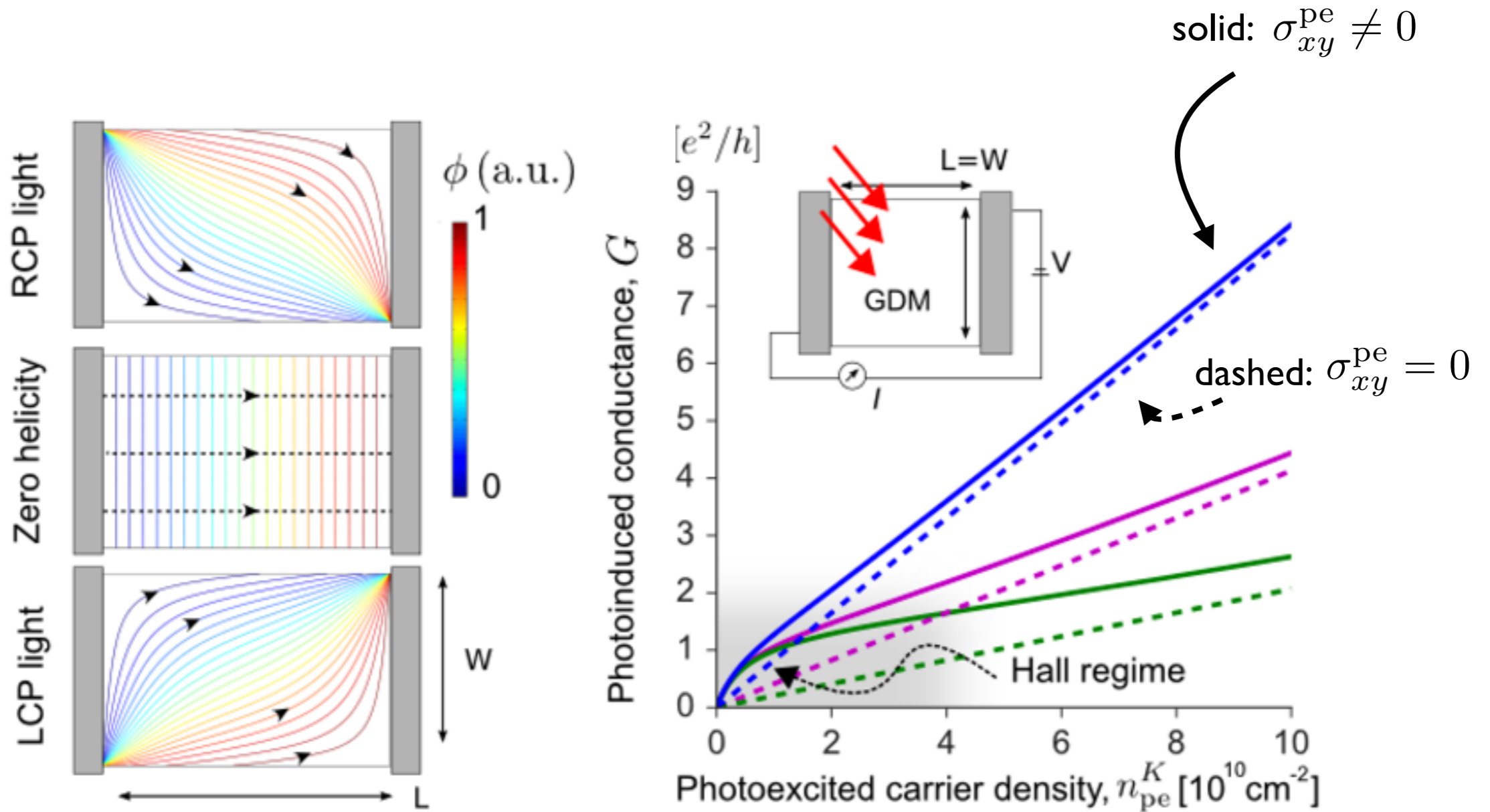


photo-resistivity is *suppressed* in
“Berry” Hall regime

Anomalous two-terminal conductance



Anomalous two-terminal conductance *boost*

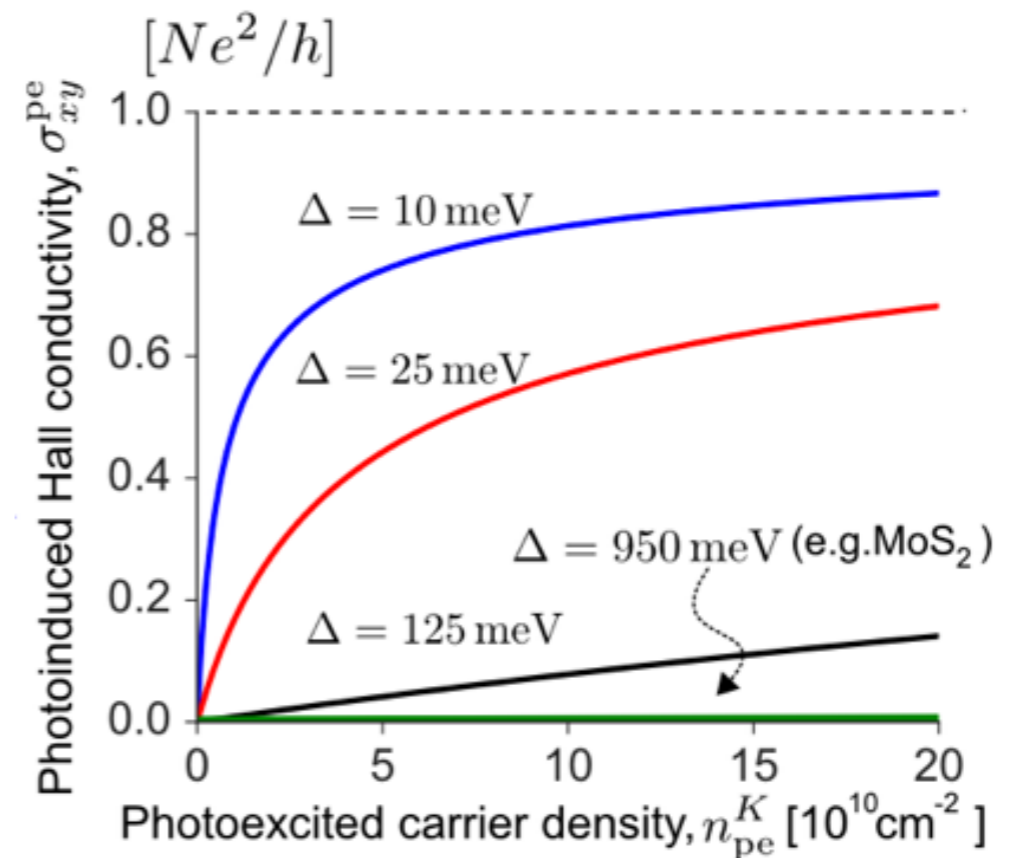


“Berry transport” in narrow GDMs

Narrow gapped Dirac materials enable
→ *giant* Hall photoconductivity

Far larger than wide gap Dirac materials.
new characteristics; readily accessible

Hall photoconductivity can overwhelm longitudinal conductivity: **Hall regime.**



Narrow gapped Dirac materials:
platform for novel “Berry” opto-electronics

In collaboration with:



Mikhail Kats
(Wisconsin)

Funding:

**NATIONAL
RESEARCH
FOUNDATION**
(Singapore)

Plan

Part I.

Giant Hall photoconductivity

gapped Dirac materials with a narrow gap yield giant Hall photoconductivity
order $\sim e^2/h$ = access to “Berry” transport regime [Hall regime]

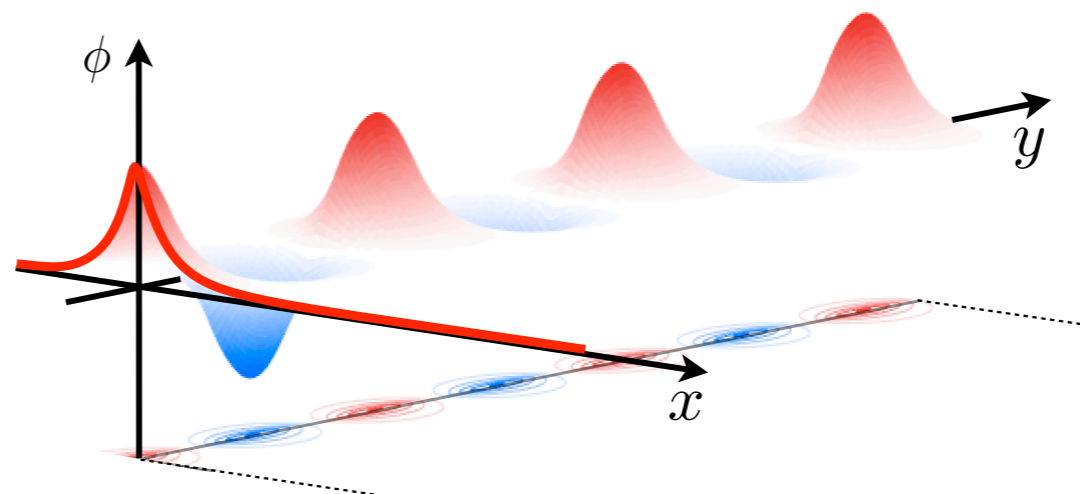
Part II.

Anomalous Plasmons

electron interactions + Berry curvature = new collective modes (“Berry Plasmons”)

Berry plasmons: JS, Rudner, PNAS (2016)

Weyl semimetals: JS, Rudner, arXiv (2017)



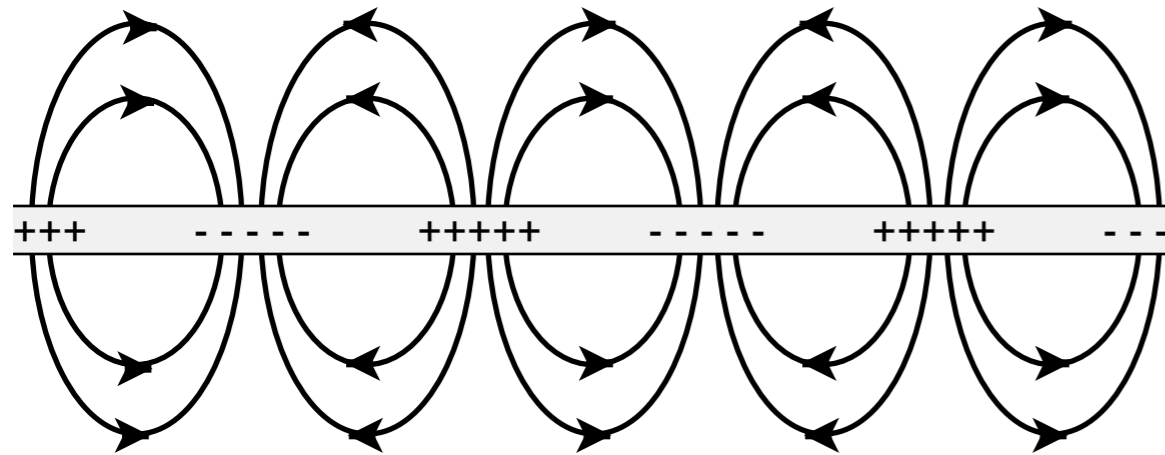
In collaboration with:



Mark Rudner
(Copenhagen)

Interactions and Collective modes

Plasmons



Spin waves/magnons

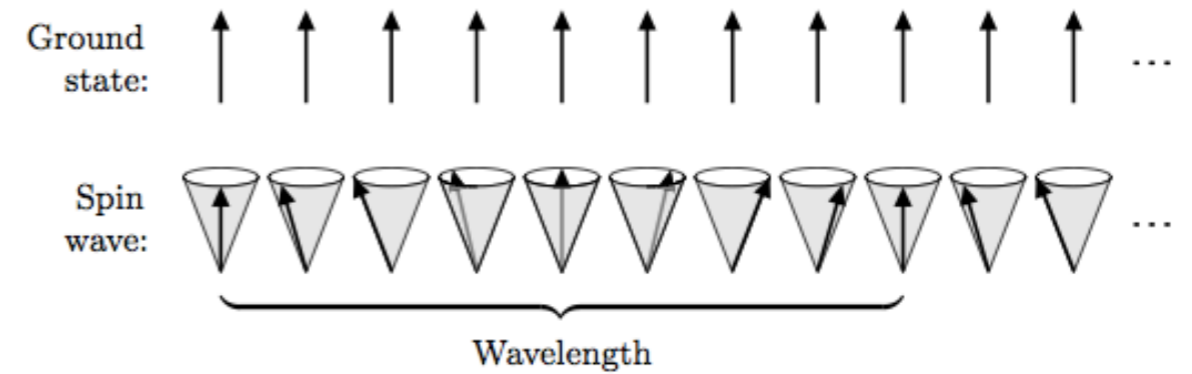
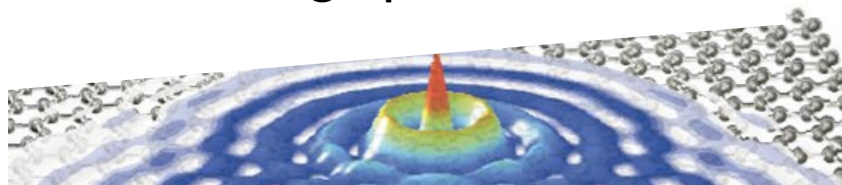


Image from <http://wikipedia.org>

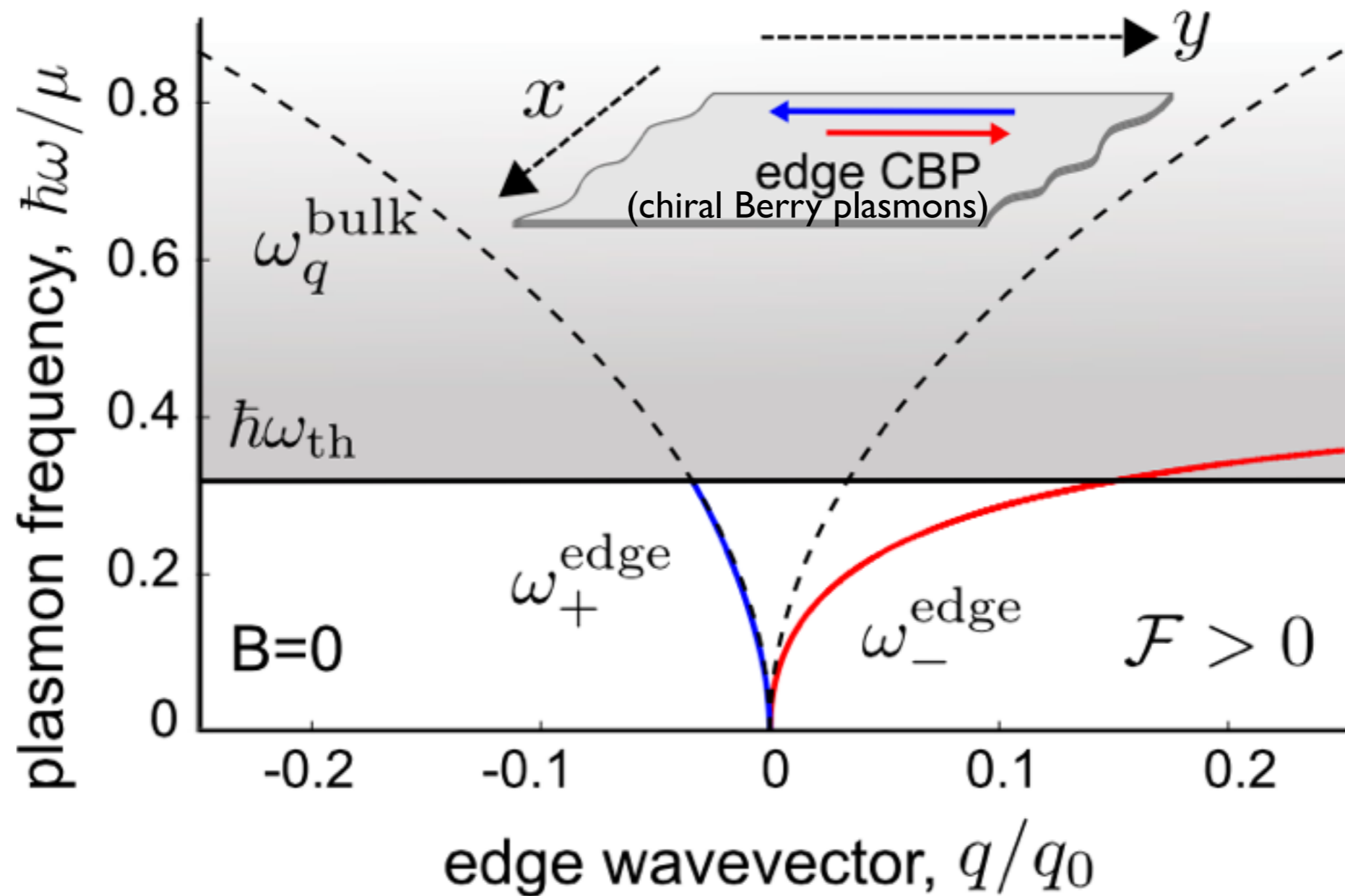
e.g. Plasmons in graphene



Koppens group, Nature (2013) Basov group Nature (2013)

Interactions + Berry curvature = Berry plasmons?

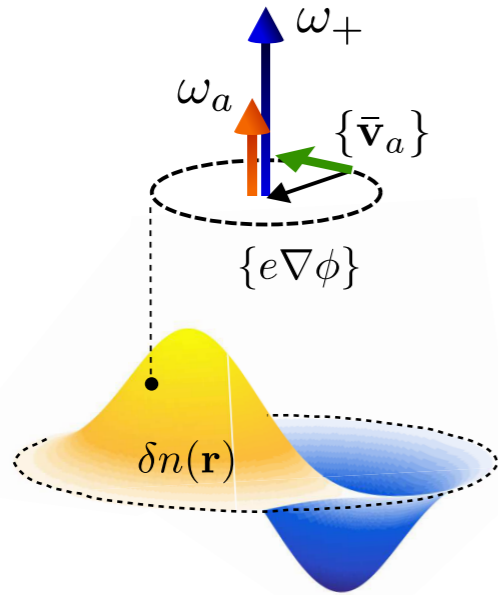
Chiral edge plasmons induced by Berry curvature



characteristic wavevector
 $q_0 = \kappa\mu/e^2$

Berry plasmons in a disk

Counter-clockwise (fast) mode



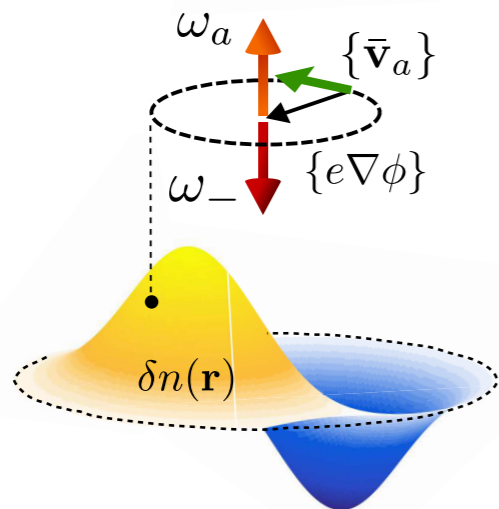
Linearized equation of motion:

$$\begin{pmatrix} \frac{d^2}{dt^2} + \omega_0^2 & -\omega_a \frac{d}{dt} \\ \omega_a \frac{d}{dt} & \frac{d^2}{dt^2} + \omega_0^2 \end{pmatrix} \begin{pmatrix} \{x(t)\} \\ \{y(t)\} \end{pmatrix} = 0 \quad \omega_a = \frac{\mathcal{F}\omega_0^2 m}{n_0 \hbar}$$

Obtain two chiral modes:

$$\{\mathbf{x}(t)\}_{\pm} = \frac{|\mathbf{x}_0|}{\sqrt{2}} \begin{pmatrix} 1 \\ \pm i \end{pmatrix} e^{i\omega_{\pm} t}, \quad \omega_{\pm} = \sqrt{\omega_0^2 + \frac{\omega_a^2}{4}} \pm \frac{\omega_a}{2}$$

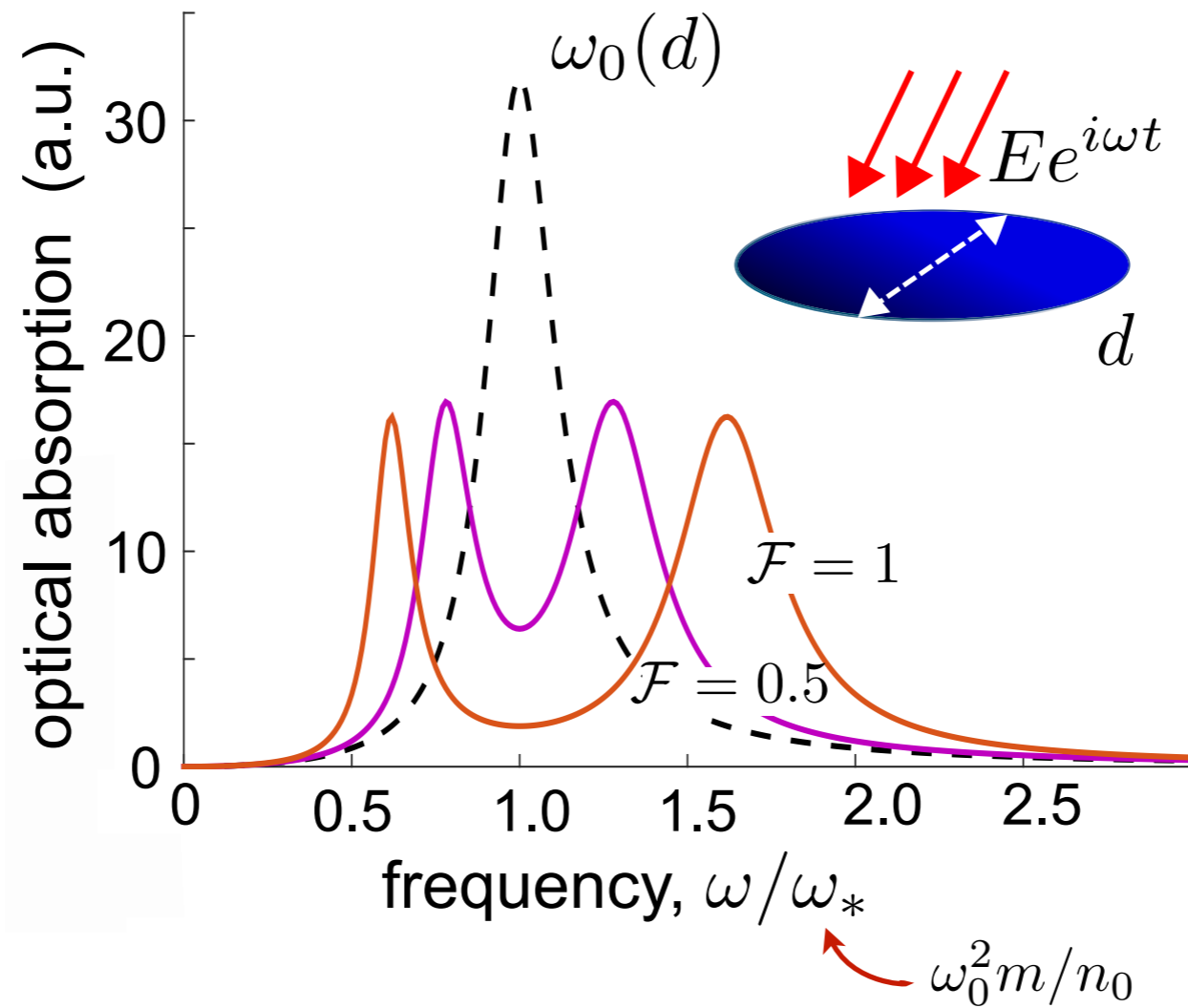
Clockwise (slow) mode



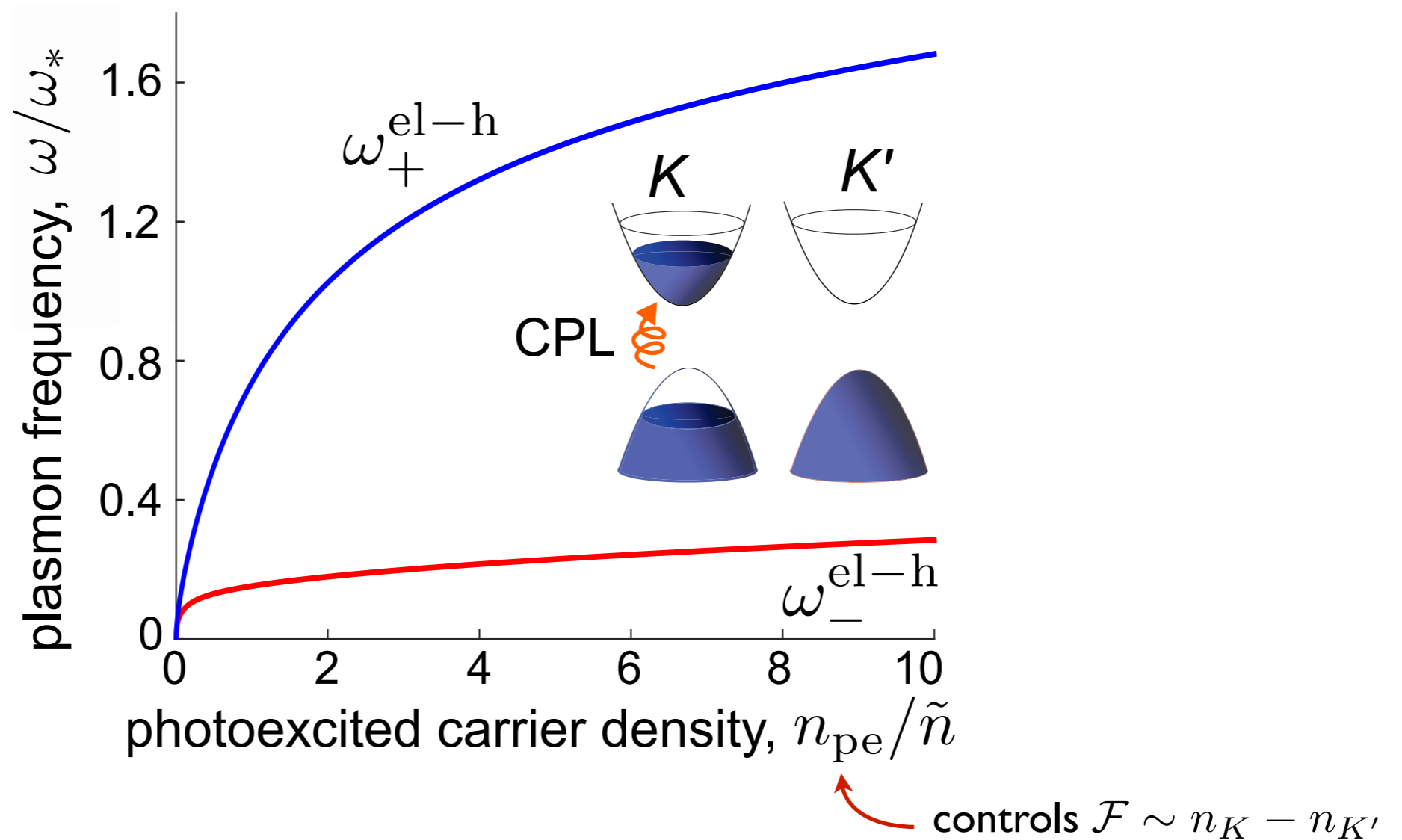
using $\omega_0 \sim \omega_{2D}(q = 1/d)$, find

$$\delta\omega \approx \frac{9\mathcal{F}}{d[\mu\text{m}]} \text{ meV}$$

Experimental signatures: optical absorption



Optical valley polarization enables CBPs “on demand” in *non-magnetic* materials (e.g., Gapped Dirac Materials)



Topological materials

Topological Insulators

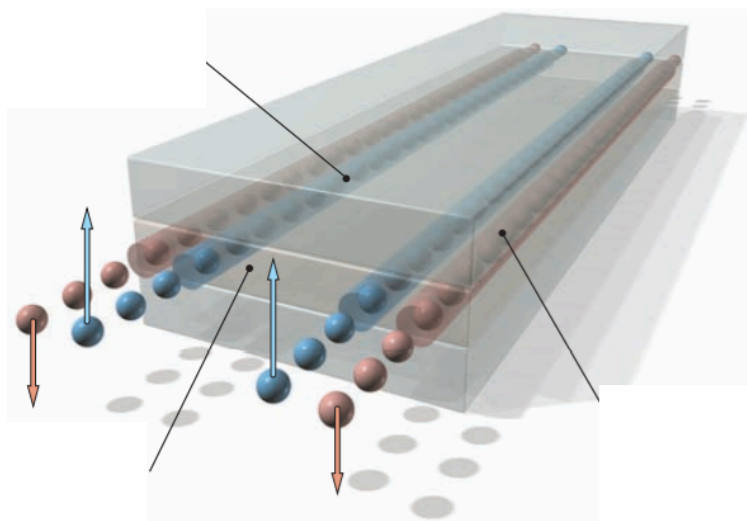
Surfaces of 3D TIs:

Bi_2Se_3 , Bi_2Te_3 , $\text{Bi}_x\text{Sb}_{1-x}$, ...

Topological Crystalline Insulators:
 SnTe , ...

Magnetic Topological Insulators:
Cr-doped BiSbTe

$\text{Hg}_x\text{Cd}_{1-x}\text{Te}$ Quantum Wells,
 InAs/GaSb QWs



3D Dirac/Weyl

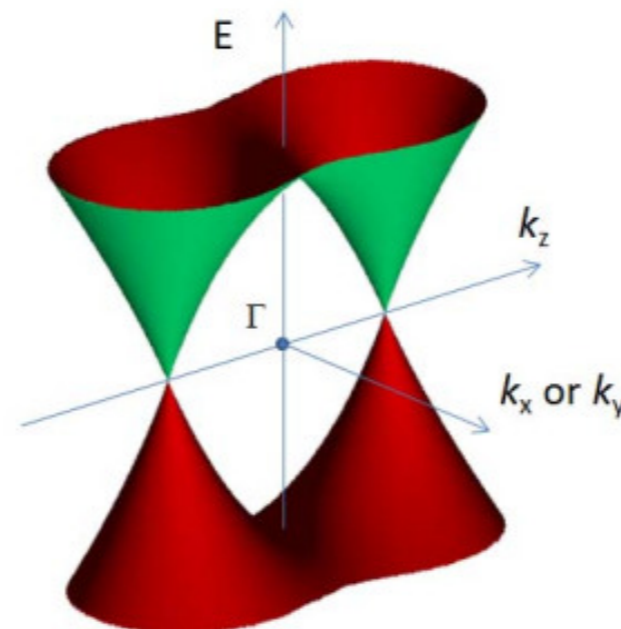
Experimentally Observed:

Cd_3As_2 , Na_3Bi , TiBiSe
 TaAs_2 , ...

Type II Weyl semimetals
(candidates): WTe_2 , MoTe_2

Proposed in TI stacks;
 HgCdTe Stacks

Nodal-line semimetals



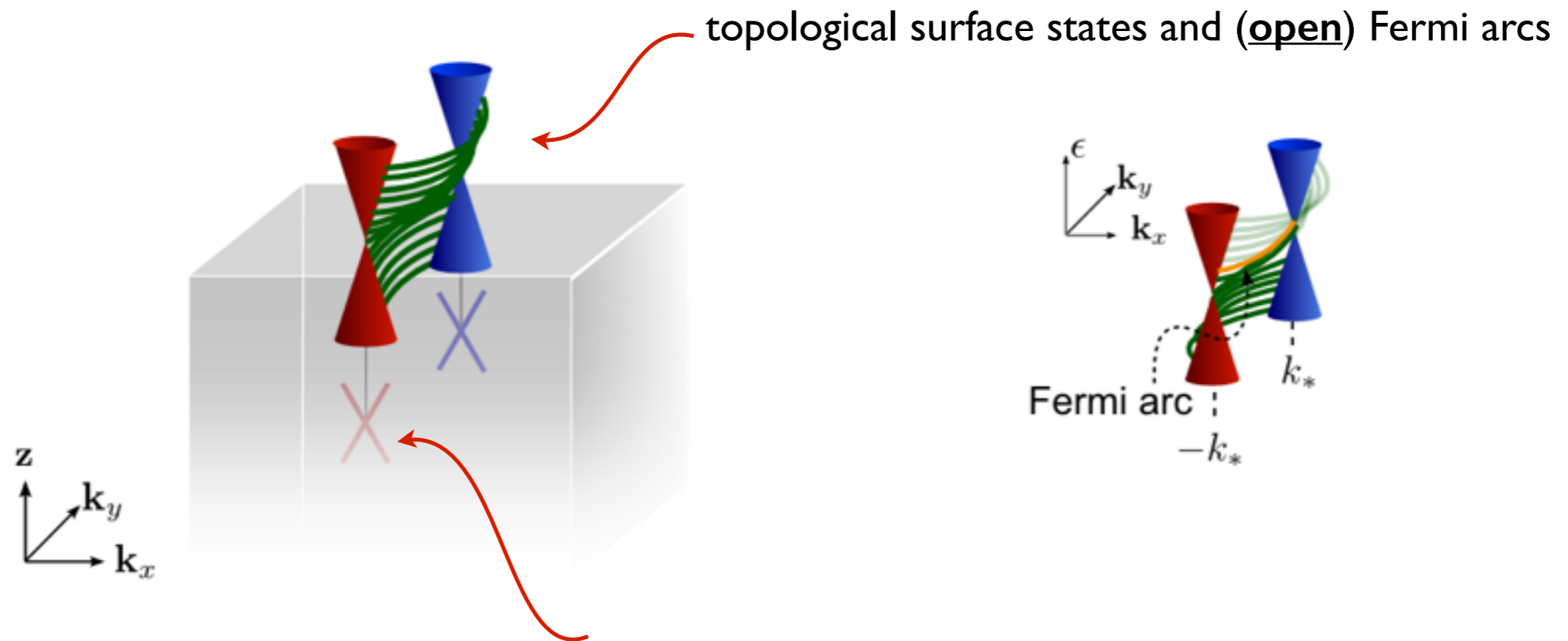
2D Dirac Materials

(materials that host Berry curvature)

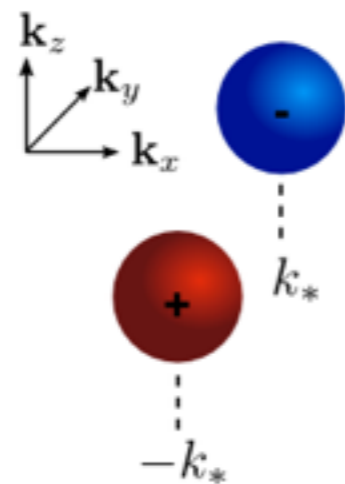
Graphene heterostructures:
 G/hBN ,
dual-gated Bilayer graphene, ...

Transition metal dichalcogenides:
 MoS_2 , WS_2 , WSe_2 , MoSe_2 ,
 MoTe_2 , ...

Weyl semimetals and Fermi arc surface states



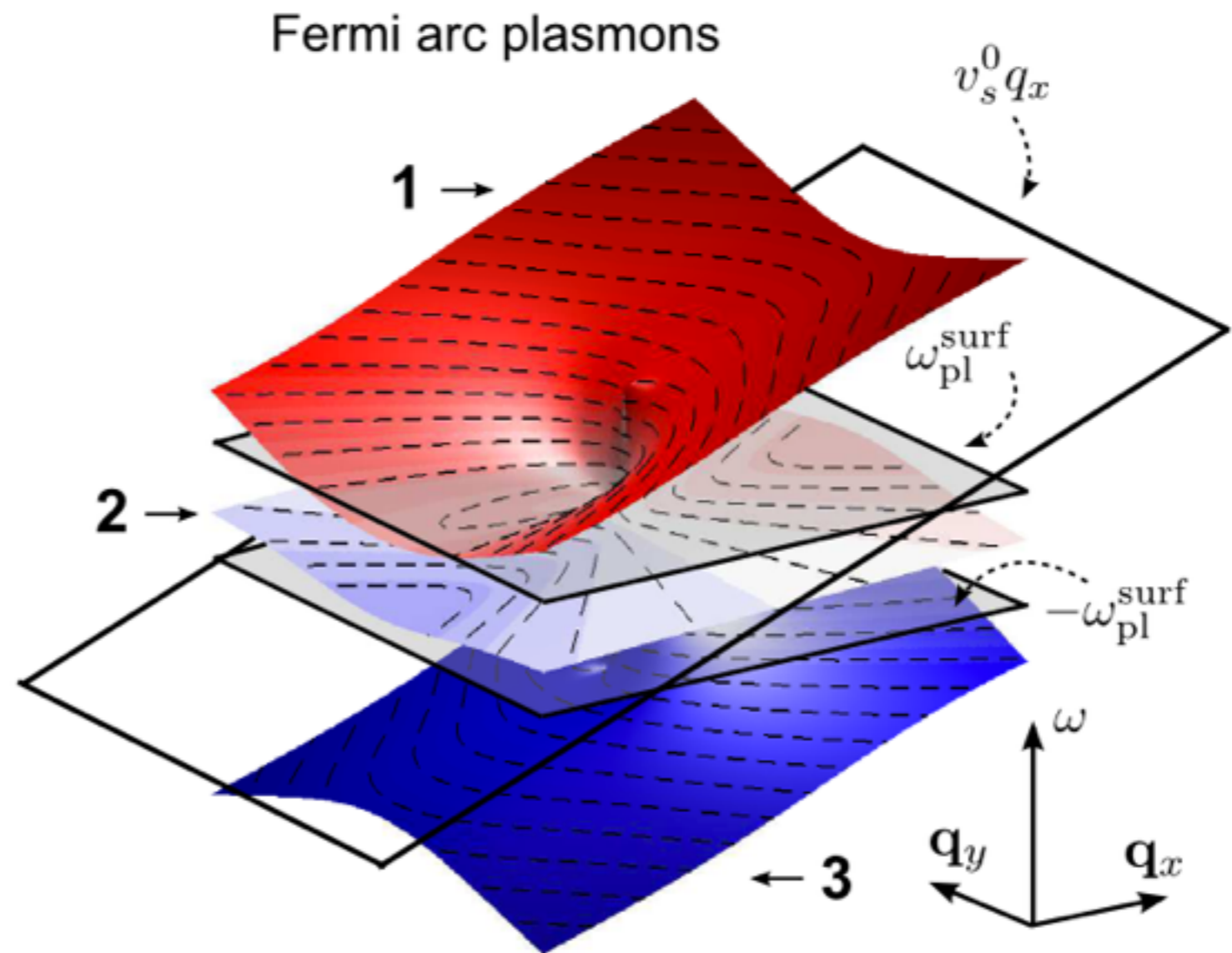
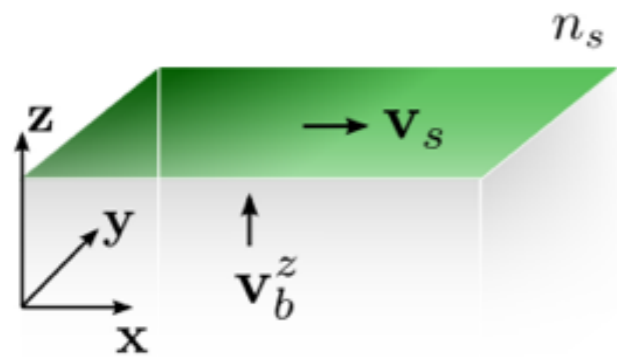
bulk Weyl nodes and bulk (closed) Fermi surface



Fermi arc plasmons in Weyl semimetals

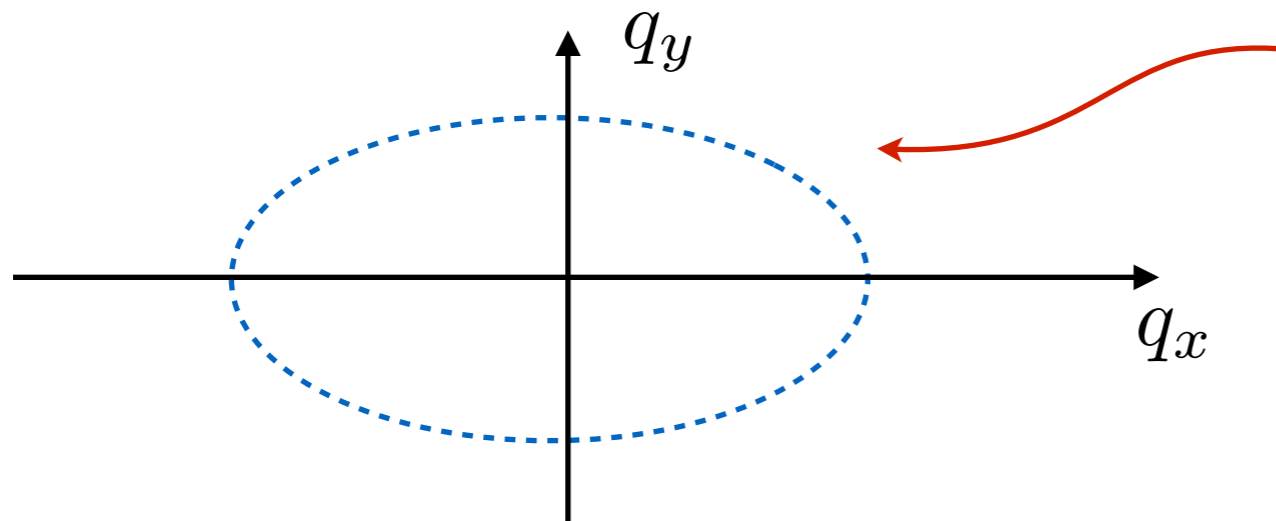
with broken TRS

inter bulk/surface[fermi-arc] dynamics



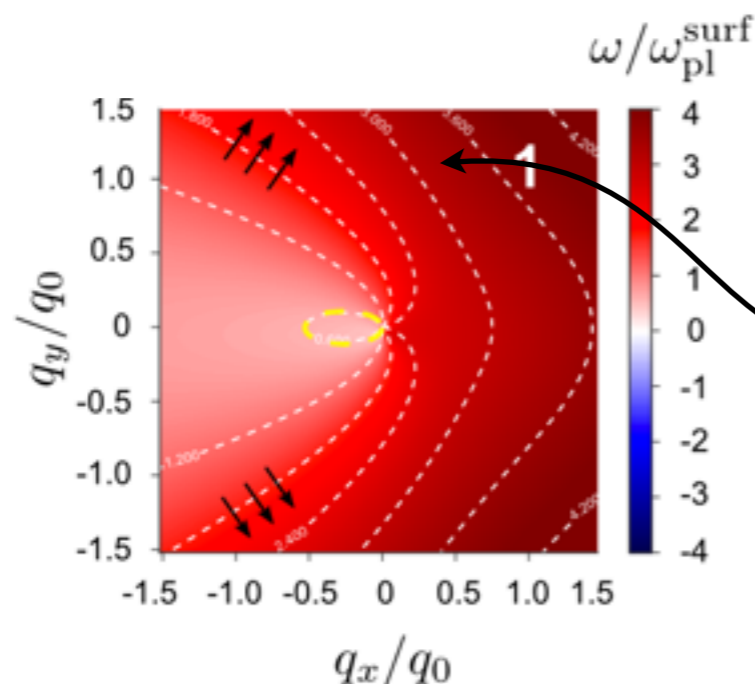
Hyperbolic plasmons

conventionally, plasmons have elliptical dispersions (closed) = **finite** wave vector magnitude



“conventional” plasmonic constant energy contour

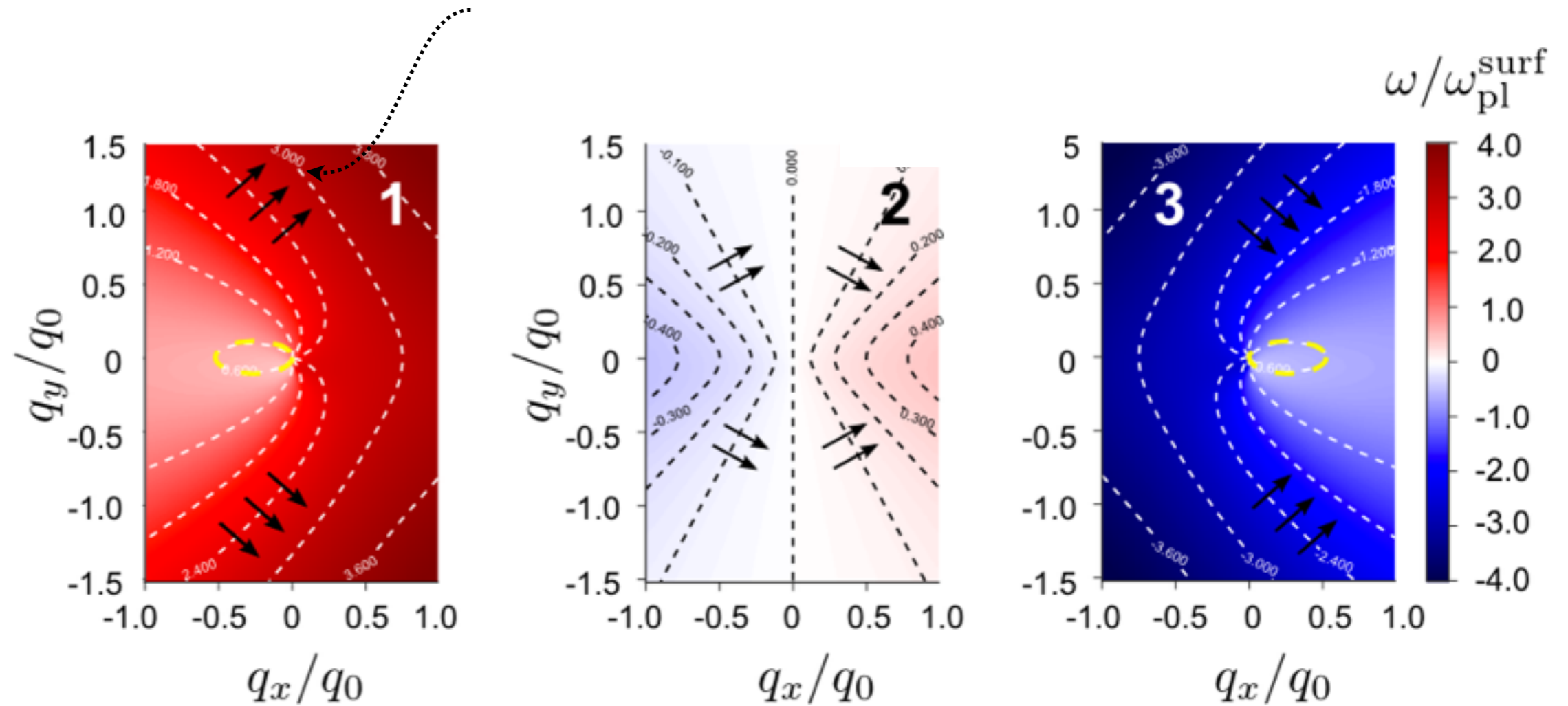
Hyperbolic dispersion does not close on itself (open) = sustain **large** wavevectors for fixed energy



“hyperbolic” plasmonic constant energy contour

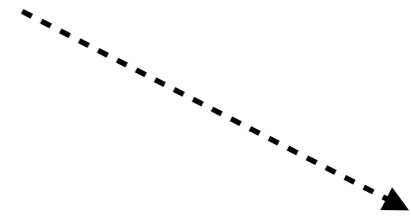
Fermi arc plasmons in Weyl semimetals

collimated plasmonic beams; FAPs intrinsically *hyperbolic*



Fermi arc plasmons

characteristic of bulk
 “topological” Weyl carrier
 dynamics



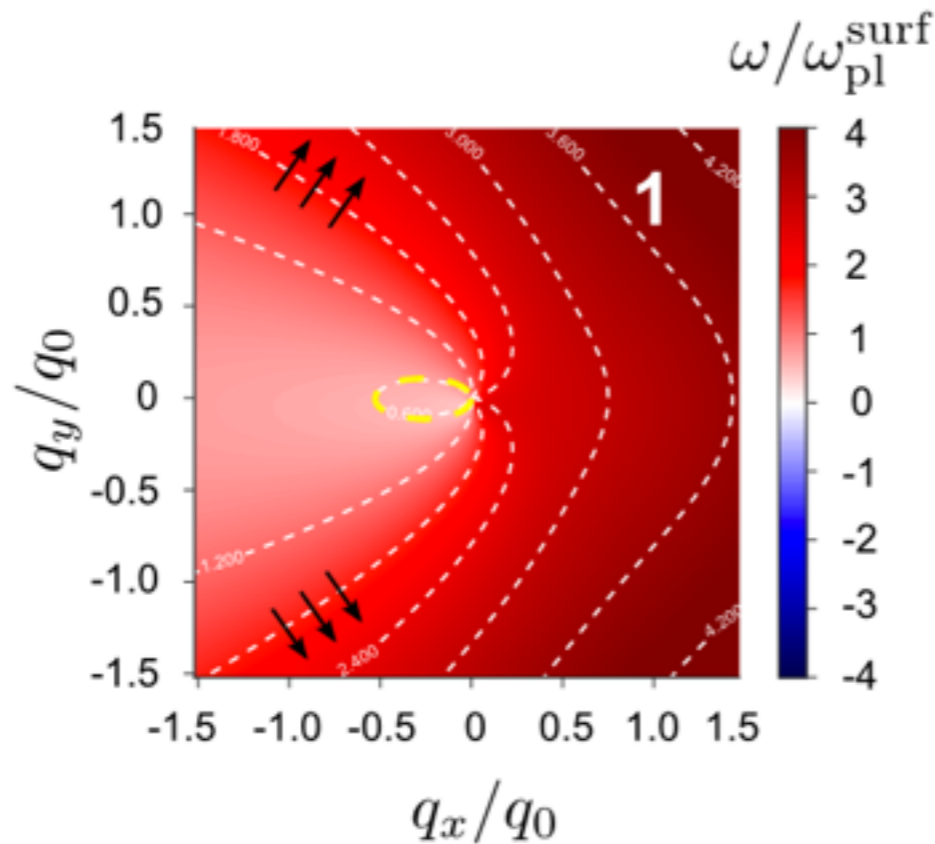
collimated beam pitch controlled by frequency:

$$\frac{\sin^2 \theta_\infty}{\cos \theta_\infty} = -\frac{\tilde{\omega}}{\tilde{D}} \left(1 - \frac{1}{\tilde{\omega}^2}\right),$$

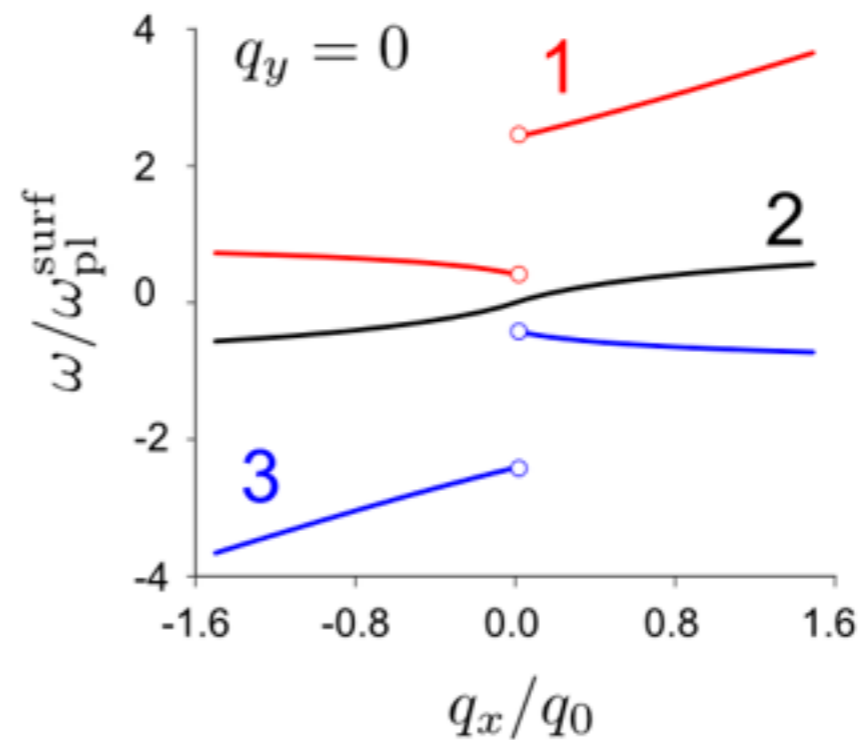
plasmon dispersion can be dominated by σ_H

$$\omega_{\pm}^{(1)} = \sqrt{\left[2\pi\sigma_H/(\kappa + 1)\right]^2 + [\omega_{\text{pl}}^{\text{surf}}]^2} \pm \frac{2\pi\sigma_H}{(\kappa + 1)},$$

large q limit: hyperbolic plasmons



small q limit: non-reciprocal discontinuity



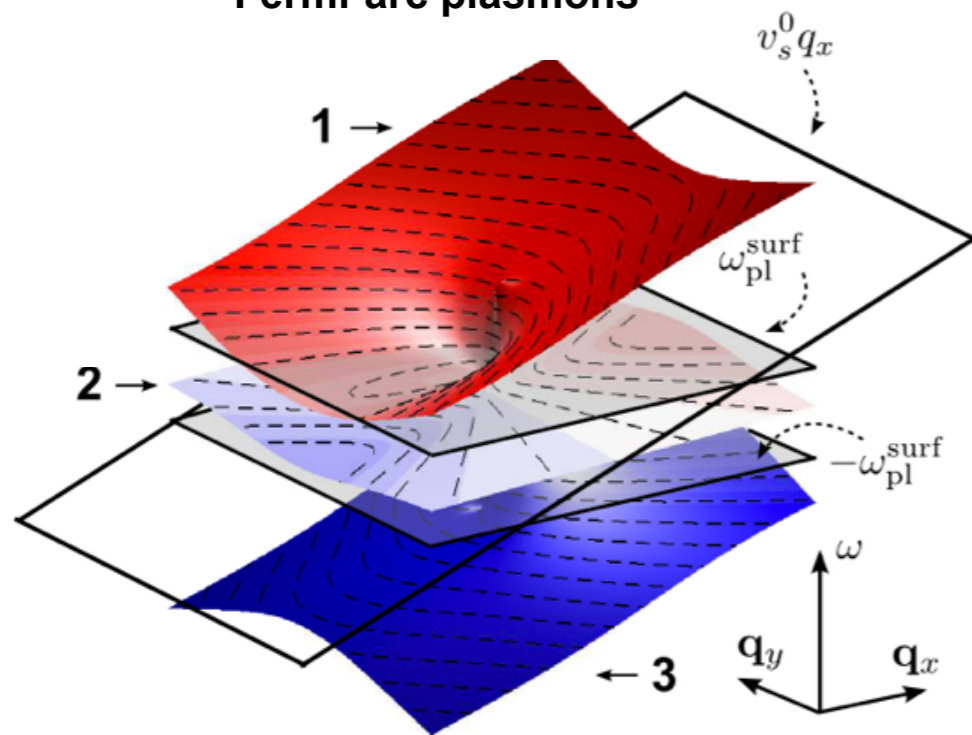
new opto-electronics in topological materials

quantum coloring: new tools, lots to be done

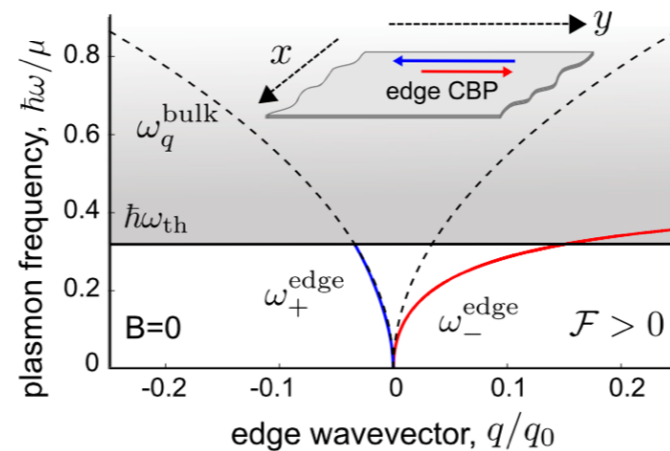
unusual properties of the crystal wave function (e.g., encoded in Berry curvature, chiral edge states) yield unconventional single-particle as well as interacting behavior

new opto-electronics couplings, and tools to be found in “topological” materials

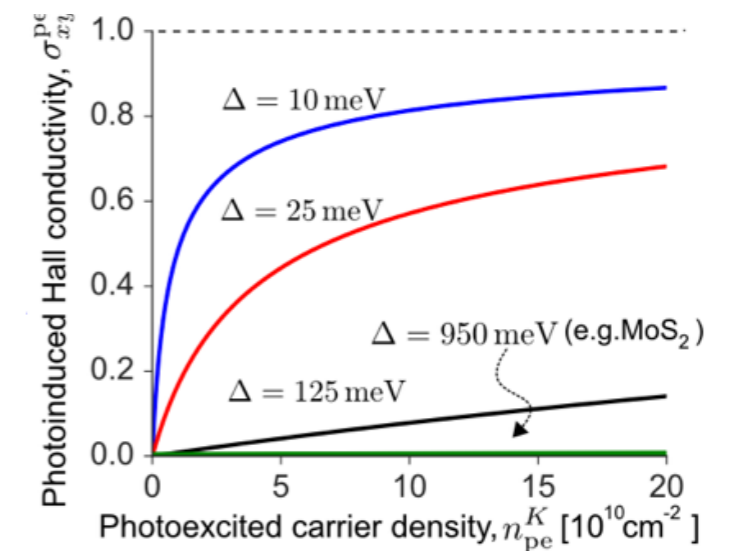
Fermi-arc plasmons



chiral edge Berry plasmons



anomalous photoconductivity



We gratefully acknowledge our Funding source:

**NATIONAL
RESEARCH
FOUNDATION**